



<https://www.nrel.gov/docs/fy09osti/44313.pdf>

Advanced Power Electronic Interfaces for Distributed Energy Systems

Part 2: Modeling, Development, and Experimental Evaluation of Advanced Control Functions for Single-Phase Utility-Connected Inverter

S. Chakraborty, B. Kroposki, and W. Kramer

Technical Report
NREL/TP-550-44313
November 2008



Advanced Power Electronic Interfaces for Distributed Energy Systems

Technical Report
NREL/TP-550-44313
November 2008

Part 2: Modeling, Development, and Experimental Evaluation of Advanced Control Functions for Single-Phase Utility-Connected Inverter

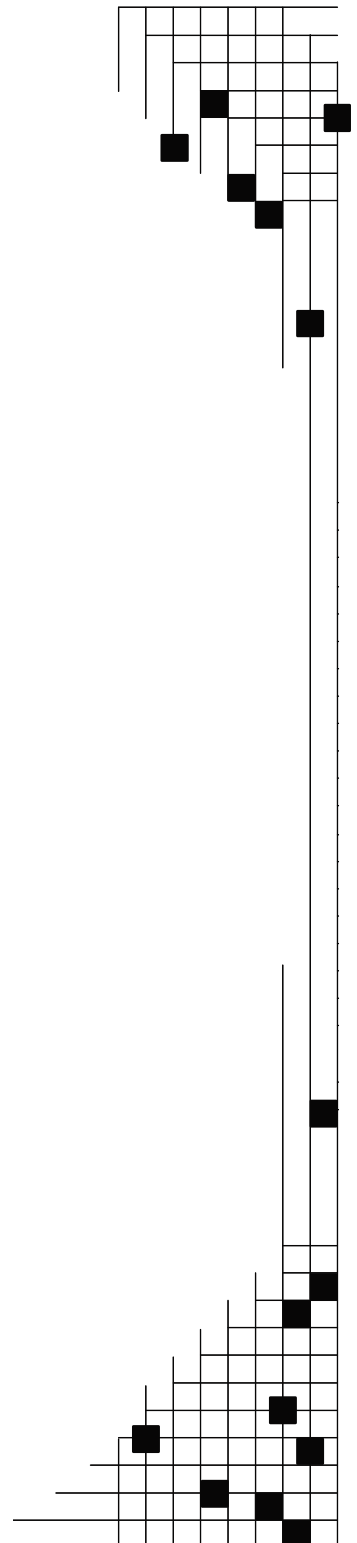
S. Chakraborty, B. Kroposki, and W. Kramer

Prepared under Task No. WW2C.1000

National Renewable Energy Laboratory
1617 Cole Boulevard, Golden, Colorado 80401-3393
303-275-3000 • www.nrel.gov

NREL is a national laboratory of the U.S. Department of Energy
Office of Energy Efficiency and Renewable Energy
Operated by the Alliance for Sustainable Energy, LLC

Contract No. DE-AC36-08-GO28308



The National Renewable Energy Laboratory is a national laboratory of the U.S. Department of Energy (DOE) managed by the Alliance for Sustainable Energy, LLC for the U.S. Department of Energy under Contract Number DE-AC36-08-GO28308. This report was prepared as an account of work sponsored by the California Energy Commission and pursuant to an M&O Contract with the United States Department of Energy (DOE). Neither the Alliance for Sustainable Energy, nor the DOE, nor the California Energy Commission, nor any of their employees, contractors, or subcontractors, makes any warranty, express or implied, or assumes any legal liability or responsibility for the accuracy, completeness, or usefulness of any information, apparatus, product, or process disclosed, or represents that its use would not infringe privately owned rights. Reference herein to any specific commercial product, process, or service by trade name, trademark, manufacturer, or otherwise, does not necessarily constitute or imply its endorsement, recommendation, or favoring by Midwest Research Institute, or the DOE, or the California Energy Commission. The views and opinions of authors expressed herein do not necessarily state or reflect those the Alliance for Sustainable Energy, the DOE, or the California Energy Commission, or any of their employees, or the United States Government, or any agency thereof, or the State of California. This report has not been approved or disapproved by the Alliance for Sustainable Energy, the DOE, or the California Energy Commission, nor has the Alliance for Sustainable Energy, the DOE, or the California Energy Commission passed upon the accuracy or adequacy of the information in this report.

NOTICE

This report was prepared as an account of work sponsored by an agency of the United States government. Neither the United States government nor any agency thereof, nor any of their employees, makes any warranty, express or implied, or assumes any legal liability or responsibility for the accuracy, completeness, or usefulness of any information, apparatus, product, or process disclosed, or represents that its use would not infringe privately owned rights. Reference herein to any specific commercial product, process, or service by trade name, trademark, manufacturer, or otherwise does not necessarily constitute or imply its endorsement, recommendation, or favoring by the United States government or any agency thereof. The views and opinions of authors expressed herein do not necessarily state or reflect those of the United States government or any agency thereof.

Available electronically at <http://www.osti.gov/bridge>

Available for a processing fee to U.S. Department of Energy and its contractors, in paper, from:

U.S. Department of Energy
Office of Scientific and Technical Information
P.O. Box 62
Oak Ridge, TN 37831-0062
phone: 865.576.8401
fax: 865.576.5728
email: <mailto:reports@adonis.osti.gov>

Available for sale to the public, in paper, from:

U.S. Department of Commerce
National Technical Information Service
5285 Port Royal Road
Springfield, VA 22161
phone: 800.553.6847
fax: 703.605.6900
email: orders@ntis.fedworld.gov
online ordering: <http://www.ntis.gov/ordering.htm>



Acronyms

AC	alternating current
A/D	analog to digital
ADC	analog to digital conversion
ANSI	American National Standards Institute
CPU	central processing unit
DC	direct current
DE	distributed energy
DER	distributed energy resource
DSP	digital signal processor
DSTATCOM	distributed static synchronous compensator
EPS	electrical power system
FACTS	flexible AC transmission systems
FY	fiscal year
GE	General Electric
GPIO	general-purpose input-output
HMI	human-machine interface
IC	integrated circuit
IDE	integrated development environment
IEEE	Institute of Electrical and Electronics Engineers
IGBT	insulated-gate bipolar transistor
IPEM	integrated power electronics module
JTAG	Joint Test Action Group
mH	milihenry
NREL	National Renewable Energy Laboratory
PCC	point-of-common-coupling
PE	power electronics
PI	proportional–integral
PID	proportional–integral–derivative
PLL	phase-locked-loop
PWM	pulse-width modulation
RAM	random access memory
RLC	resistive, inductive and capacitive
RMS	root mean square
s	second
SKAI	Semikron advanced integration
STATCOM	static synchronous compensator
THD	total harmonic distortion
TI	Texas Instrument
uF	microfarad
UPF	unity power factor
VAR	volt-amperes reactive

Table of Contents

1	Executive Summary	1
2	Introduction	2
3	Modeling and Simulation	3
3.1	Power Circuit	3
3.2	Basic Inverter Control.....	5
3.3	Power Flow Control.....	11
3.4	VAR/Voltage Control	14
4	Hardware Testing	21
4.1	Hardware Setup.....	21
4.2	Experimental Results	26
5	Rapid Control Prototyping	40
5.1	Voltage and Current Control.....	40
5.2	Power Flow Control.....	47
5.3	VAR/Voltage Control	50
6	Conclusion	53
	References	54

List of Figures

Figure 1.	Power Circuit for Complete Inverter System.....	4
Figure 2.	Block Diagram of Voltage Control Loop	5
Figure 3.	Block Diagram of Current Control Loop.....	6
Figure 4.	Simulation Results for Current Control Mode of Operation	8
Figure 5.	Simulation Results for Voltage Control Mode of Operation	9
Figure 6.	Simulation Waveforms for Complete Inverter Operation	10
Figure 7.	Block Diagram of Power Flow Control Loop.....	12
Figure 8.	Active and Reactive Power Waveforms for Power Flow Control	12
Figure 9.	Voltage and Current Waveforms for Power Flow Control.....	13
Figure 10.	Active and Reactive Power for Step Change in Power Commands	14
Figure 11.	Power Circuit for VAR Control System	16
Figure 12.	Block Diagram of VAR/Voltage Controller	17
Figure 13.	Voltage and Current Waveforms for VAR/Voltage Control	18
Figure 14.	Active and Reactive Power Waveforms for VAR/Voltage Control	19
Figure 15.	Simulation Waveforms of VAR/Voltage Control for Second Case	20
Figure 16.	Picture of Front Side of Inverter Platform	22
Figure 17.	Detailed Power Circuit Diagram and Connections (Drawn in P-CAD)	23
Figure 18.	Picture of Control Board with Input/Output Connections	24
Figure 19.	Single Line Diagram of Test Setup.....	25
Figure 20.	Inverter Voltage Control Experiment	27
Figure 21.	Voltage Regulation of the Voltage-Controlled Inverter	27
Figure 22.	Efficiencies of the Voltage-Controlled Inverter	28
Figure 23.	Inverter Current Control (Case 1).....	29
Figure 24.	Inverter Current Control (Case 2).....	30
Figure 25.	Harmonic Analysis by Yokogawa Scope	31
Figure 26.	Voltage Regulation of the Current-Controlled Inverter.....	32
Figure 27.	Efficiencies of the Current-Controlled Inverter	32
Figure 28.	Inverter Power Flow Control (P=1200W, Q=0)	34
Figure 29.	Inverter Power Flow Control (P=0W, Q=1100VAR).....	34
Figure 30.	Inverter Power Flow Control (P=700W, Q=± 700VAR).....	35
Figure 31.	VAR/Voltage Control (Local Load 12 Ohm).....	37
Figure 32.	VAR/Voltage Control (Local Load 8 Ohm)	38
Figure 33.	VAR/Voltage Control (Local Load 20 Ohm).....	39
Figure 35.	Structure of the Voltage Control Subsystem	44
Figure 36.	Structure of the Current Control Subsystem.....	44
Figure 37.	Voltage Control at No Load.....	45
Figure 38.	Voltage Control at Full Load	46
Figure 39.	Current Control	46
Figure 40.	Complete Control Structure for the Voltage and Power Flow Control	48
Figure 41.	Power Flow Control (P=800W, Q=-800VAR).....	49
Figure 42.	Power Flow Control (P=900W, Q=800VAR)	49
Figure 43.	Complete Control Structure for the Voltage and VAR Control	51
Figure 44.	VAR/Voltage Control (Local Load 10 Ohm).....	52

1 Executive Summary

Power electronics (PE) are integral components of renewable and distributed energy (DE) systems. Successful Smart Grid implementation requires that electricity customers have the advanced technology tools and information needed to participate in the market. Developing interoperable, intelligent technology devices—such as advanced PE technology that will improve and accelerate the use of distributed energy resource (DER) systems is key to successful Smart Grid implementation. In addition to the common power conversion functions, the value of PE can be greatly enhanced by developing advanced control functionalities such improved power quality, voltage/volt-amperes reactive (VAR) support, reduced DE fault contributions, and flexible operation with various DE sources (Kroposki et al. 2006). Working with project partners (Northern Power Systems, GE, and the California Energy Commission), the National Renewable Energy Laboratory (NREL) is modeling, developing, and evaluating advanced power electronics topologies and controls to achieve PE systems that are reliable, energy efficient, and cost competitive. The main objective of this task was to develop and test advanced single-phase inverter controls that would allow DE systems to provide ancillary services such as power flow control and VAR/voltage regulation to the power distribution system. Fast prototyping techniques together with modular PE devices will lead to easier, low-cost implementation and prototyping of the DE interfaces.

In fiscal year 2007 (FY07), NREL developed a generic single-phase DC-AC inverter platform based on a Semikron SKAI module and an F2812 eZdsp controller and conducted some initial testing of the inverter platform (Chakraborty et al. 2007). Also in FY07, NREL developed electrical models for generic insulated-gate bipolar transistor (IGBT)-based interfaces that can be used across multiple DE platforms. Electric loads and electric system components were also modeled to complete the system. NREL then conducted validation testing to verify the electrical models of DE power electronic interfaces, electrical loads, and electrical power system (EPS) components (Chakraborty et al. 2007). In FY08, the laboratory inverter platform was modified and advanced control functionalities were developed, built, and tested using the inverter platform. These advanced PE interfaces can ensure that DE resources not only supply energy for critical site or building functions during a utility grid outage but also enhance power quality and grid support during other abnormal events. As part of the NREL work, researchers developed a simulation model. The model provides a platform for developing control methodologies of the various functions before they are implemented in the actual hardware. The inverter hardware was subjected to various transients to evaluate the system's dynamic performance and compared to the model results. Researchers identified differences between the tested and modeled system performance and the models were fine-tuned accordingly.

2 Introduction

Power electronics (PE) are integral components of renewable and distributed energy (DE) systems. Successful Smart Grid implementation requires that electricity customers have the advanced technology tools and information needed to participate in the market. Developing interoperable, intelligent technology devices—such as advanced PE technology that will improve and accelerate the use of distributed energy resource (DER) systems is key to successful Smart Grid implementation. In addition to the common power conversion functions, the value of PE can be greatly enhanced by developing advanced control functionalities such improved power quality, voltage/volt-amperes reactive (VAR) support, reduced DE fault contributions, and flexible operation with various DE sources (Kroposki et al. 2006). Working with project partners (Northern Power Systems, GE, and the California Energy Commission), the National Renewable Energy Laboratory (NREL) is modeling, developing, and evaluating advanced power electronics topologies and controls to achieve PE systems that are reliable, energy efficient, and cost competitive. The main objective of this task was to develop and test advanced single-phase inverter controls that would allow DE systems to provide ancillary services such as power flow control and VAR/voltage regulation to the power distribution system. Fast prototyping techniques together with modular PE devices will lead to easier, low-cost implementation and prototyping of the DE interfaces.

In fiscal year 2007 (FY07), NREL developed a generic single-phase DC-AC inverter platform based on the Semikron SKAI module and an F2812 eZdsp controller and conducted some initial testing of the inverter platform (Chakraborty et al. 2007). Also in FY07, NREL developed electrical models for generic insulated-gate bipolar transistor (IGBT)-based interfaces that can be used across multiple DE platforms. Electric loads and electric system components were also modeled to complete the system. NREL then conducted validation testing to verify the electrical models of DE power electronic interfaces, electrical loads, and electrical power system (EPS) components (Chakraborty et al. 2007). In FY08, the laboratory inverter platform was modified and advanced control functionalities were developed, built, and tested using the inverter platform. These advanced PE interfaces can ensure that DE resources not only supply energy for critical site or building functions during a utility grid outage but also enhance power quality and grid support during other abnormal events. As part of the NREL work, researchers developed a simulation model. The model provides a platform for developing control methodologies of the various functions before they are implemented in the actual hardware. The inverter hardware was subjected to various transients to evaluate the system's dynamic performance and compared to the model results. Researchers identified differences between the tested and modeled system performance and the models were fine-tuned accordingly.

This report is organized into three main technical sections to include modeling and simulation, hardware testing, and control development. In Section 3 of the report, modeling and simulation results for the single-phase inverter with advanced controls are described. As one of the main goals for this research is to use new methods to implement flexible, easy-to-prototype controllers; we selected MathWorks' Simulink software platform as it presents unique capabilities to model PE and control and develop digital signal processor (DSP) codes under the same platform (MathWorks Simulink 2008). The experimental validation of the advanced control objectives are provided in Section 4 along with brief details on the

hardware and control implementation. For this section all control codes are written using the C software programming language together with Texas Instrument's Code Composer Studio (Texas Instrument). The results of using this platform to prove the effectiveness of this control design approach for implementing fast control prototypes using Simulink DSP toolboxes are provided in Section 5.

3 Modeling and Simulation

For renewable energy sources that generate direct current (DC) power, an inverter is required to convert DC into alternating current (AC) for utility connection and consumer use. For low voltage levels such as 120V AC/240V AC, single-phase inverters are very common and available from different manufacturers. These commercial inverters mainly work as a controlled current source when operating in the utility-connected mode. To implement and test new controls such as VAR/voltage regulation, and to increase grid reliability in the transition from grid-tied to islanded operation modes, NREL developed a single-phase inverter hardware platform as detailed in the previous report (Chakraborty et al. 2007). In the present modeling work, we used MathWorks' Simulink SimPowerSystems to model a single-phase inverter and test inverter control algorithms before actually implementing them in the hardware (MathWorks SimPowerSystems 2008). The parameters and simulation conditions for the model were carefully selected so that it accurately emulated the hardware. Also, the control designs were developed in such a way that they can be easily implemented in the hardware DSP platform. As one of the main goals for this research is to use new methods to implement flexible, easy-to-prototype controllers; Simulink was chosen since it presents unique capabilities for developing control algorithms, modeling power electronics, and implementing DSP codes under the same software platform.

3.1 Power Circuit

The power circuit for the complete inverter system is shown in Figure 1. The DC input stage of the inverter consists of a 300V DC source along with a small series resistance of 0.4Ω . This series resistance is required in order to facilitate convergence of the model in the Simulink environment. The power electronics devices are modeled based on the Semikron SKAI module parameters used in the hardware setup. The SKAI module consists of six IGBT switches along with 1mF of input capacitor. The output of the inverter is fed to the inductor-capacitor (LC) line filter. The series-connected, 0.5mH inductors and parallel, 40uF capacitors are used in order to achieve desired voltage and current ripple characteristics. The output of the inverter is a single-phase, 60 Hz, 120V AC rms waveform.

The test setup includes: the inverter; a 120V, 60Hz AC source that emulates the utility grid; and two sets of resistances representing the utility load and the local load. The inverter, utility, and the local loads are connected to each other through three single-phase breakers. When all three breakers are closed; the inverter operates in the utility-connected mode. In that scenario, both the inverter and utility provide power to the utility load and local load. To simulate islanded operation of the inverter, the utility breaker is opened and the other two breakers remain closed so that the inverter supplies power to the local load.

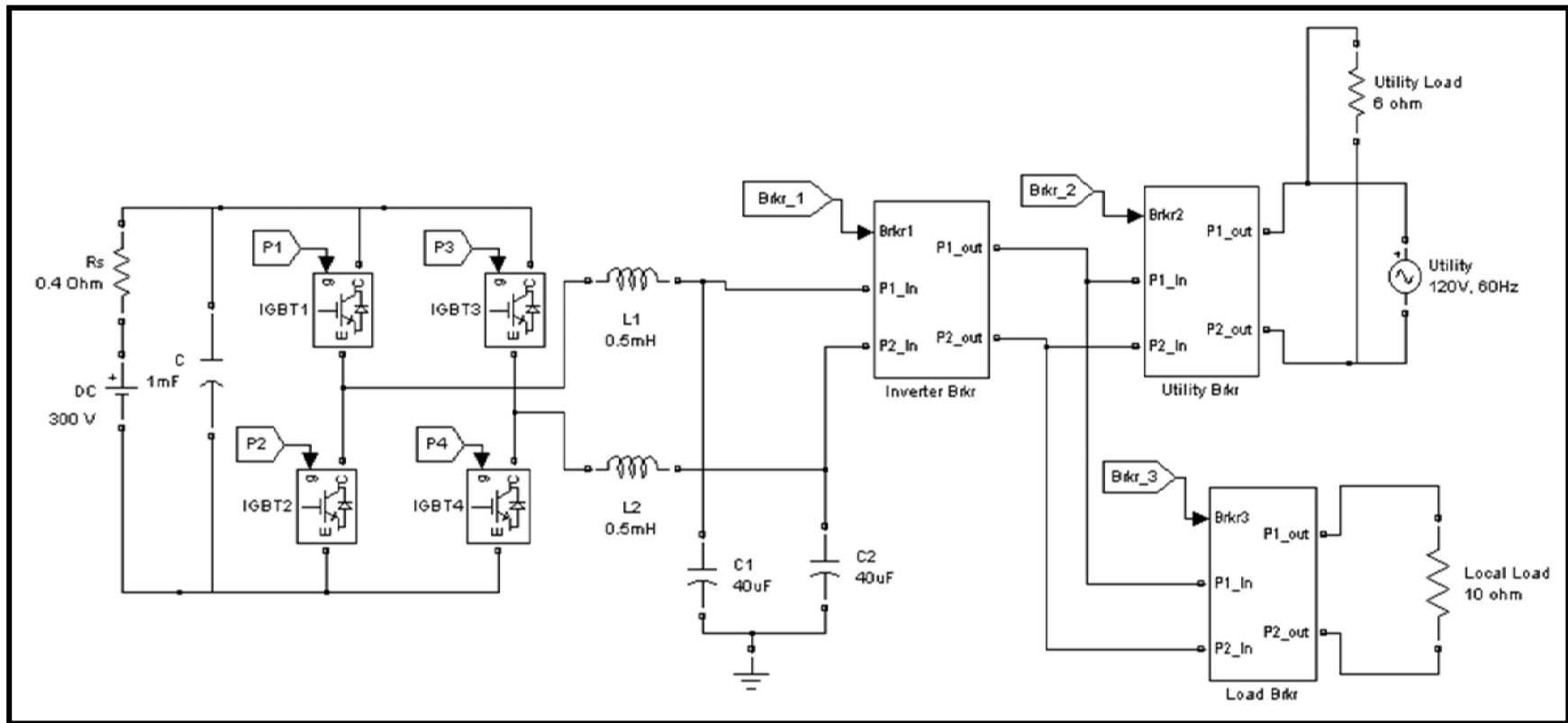


Figure 1. Power Circuit for Complete Inverter System

3.2 Basic Inverter Control

The basic inverter controls can be broadly classified into two types: current control and voltage control. When the inverter is connected to the utility, the grid controls the amplitude and frequency of the inverter output voltage and the inverter itself operates in the current control mode. Other types of inverter controls such as power flow control and VAR/voltage control can be derived from the basic current control. In contrast, in case of grid failure (grid faults, maintenance, etc.), the connected loads have to be supplied by the inverter. In such a scenario, which is often referred to as islanded operation, the inverter has to maintain the amplitude and the frequency of the voltage so that the connected loads are not affected by the utility interruption. The inverter operates in voltage control mode for such scenario providing the reference voltage and frequency.

Voltage Control

For the voltage control mode, the IGBT switches are controlled using bipolar pulse-width modulation (PWM) switching such that the inverter output voltage follows the reference voltage. The Simulink voltage control loop block diagram is shown in Figure 2. An external voltage signal with 120V AC, 60Hz is first fed into a discrete single-phase phase-locked-loop (PLL). The gain at the input of PLL is used to normalize the actual voltage signal. The output of the PLL block generates a phase angle ($\theta = \omega t$). The phase angle together with the AC voltage setpoint (V_{ac_set}) is used to generate the reference voltage, V_{ref} . The PLL is necessary to make sure that when utility voltage is present, although inverter is operating in islanded mode, the inverter voltage is synchronized with the utility voltage.

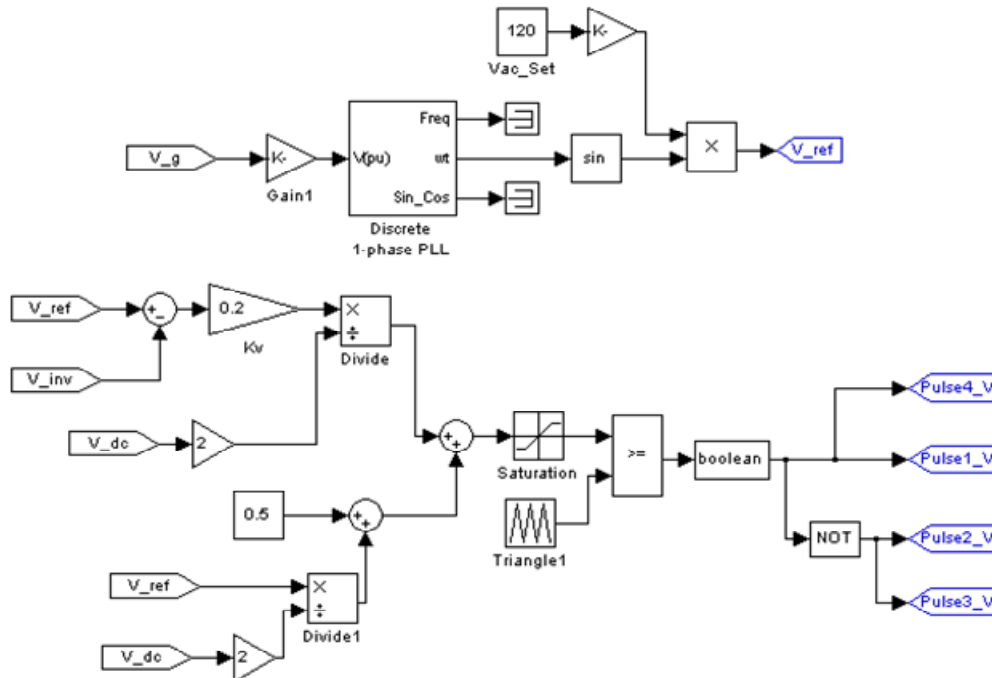


Figure 2. Block Diagram of Voltage Control Loop

In conventional PWM generation schemes, a sinusoidal control signal is compared to a triangular carrier signal to generate the PWM pattern. In order to emulate hardware DSP-

based PWM generation, we used a different control method. We compared the actual voltage to the reference signal and the error was then fed to a proportional controller. The output of the controller was then scaled and added to a feed forward loop. The final output of the controller is a duty cycle value (D), as given by equation (1).

$$D = \left(0.5 + \frac{V_ref}{2 * V_dc} \right) + \frac{Kv * (V_ref - V_inv)}{2 * V_dc} \quad (1)$$

where, V_ref is the reference voltage, V_inv is the inverter output voltage, V_dc is the input DC voltage and Kv is the proportional gain.

This duty cycle, D, is computed and then compared to a 10kHz triangular wave to generate a 10kHz PWM switching signal with positive duty cycle of D. Based on the PWM switching pattern, IGBT switches are turned on and off in a bipolar fashion, such that two diagonally opposite switches in the H-bridge turn on and off simultaneously (Mohan et al. 2003).

Current Control

In the utility-connected mode, the inverter operates as a current-controlled source to generate an output current based on a reference current signal. The Simulink block diagram of the current control loop is shown in Figure 3. Similar to the voltage control loop, a discrete PLL is used to find the phase angle of the utility voltage. The user defined rms current amplitude (Iac_Set) and phase angle (Phase_Set) are then used to generate the reference current waveform.

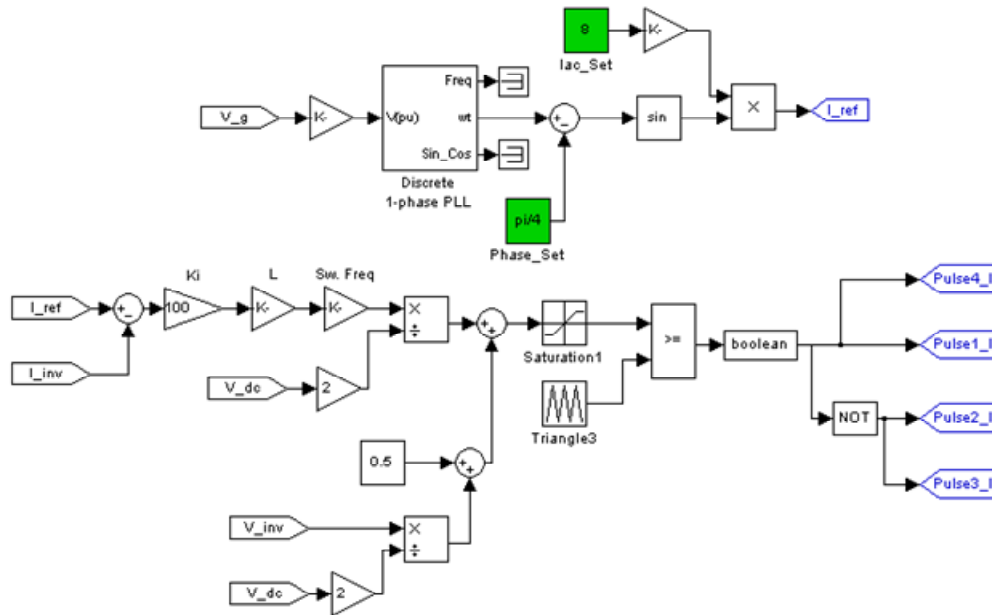


Figure 3. Block Diagram of Current Control Loop

The final output of the current controller is a duty cycle value (D), and is given by equation (2).

$$D = \left(0.5 + \frac{V_{inv}}{2 * V_{dc}} \right) + \frac{K_i * (I_{ref} - I_{inv}) * L * f_{sw}}{2 * V_{dc}} \quad (2)$$

where, V_{inv} is the inverter output voltage, V_{dc} is the input DC voltage, I_{ref} is the reference current, I_{inv} is the inverter output current, K_i is the proportional gain, L is the gain and is set to a filter inductance of 500 mH, and f_{sw} is the gain equal to a switching frequency of 10 kHz.

As with the voltage control loop, this duty value is then compared to a 10kHz triangular wave to generate a 10kHz PWM switching signal with positive duty cycle of D.

Simulation Results for Voltage and Current Control

The inverter model is simulated in Simulink SimPowerSystems to allow researchers to observe both voltage and current control. In the simulation, the inverter is turned on at time=0.05s in current control mode. The rms value of the reference current is set to 8A and the phase angle is set to zero degrees. In the current control mode, all three breakers are closed and the inverter operates in utility-connected mode. At 0.5s, the utility breaker is opened, thus transforming the inverter control to voltage control to maintain 120V, 60Hz AC voltage to the local load. Finally the inverter is turned off at 0.95s. During the simulation, the local load is set as 10 Ω resistive and the utility load is set at 6 Ω resistive.

The simulation results for current control mode are shown in Figure 4. The waveforms for the inverter voltage (V inverter), inverter current (I inverter), utility voltage (Vs), and utility current (Is) are given in Figures 4 (a)–(d). We can observe from these figures that the waveforms are very clean with only some higher order current harmonics present in the inverter current waveform.

During utility connected mode, the inverter supplies current equal to the reference current. The local load requires 12A current, of which 8A are supplied by the inverter and the remaining 4A are delivered from the utility through point-of-common-coupling (PCC). The PCC voltage and currents are denoted by V_g and I_g respectively. Before the inverter is turned on, all breakers are opened, and the utility supplies 20A rms to the utility load. When the inverter is operating, the utility supplies its own load along with the residual current required by the local load. The rms calculations for the currents are shown in Figures 4 (e)-(h). The simulation suggests that the inverter current control loop does a very good job of maintaining an 8A rms current when operated in the utility connected mode.

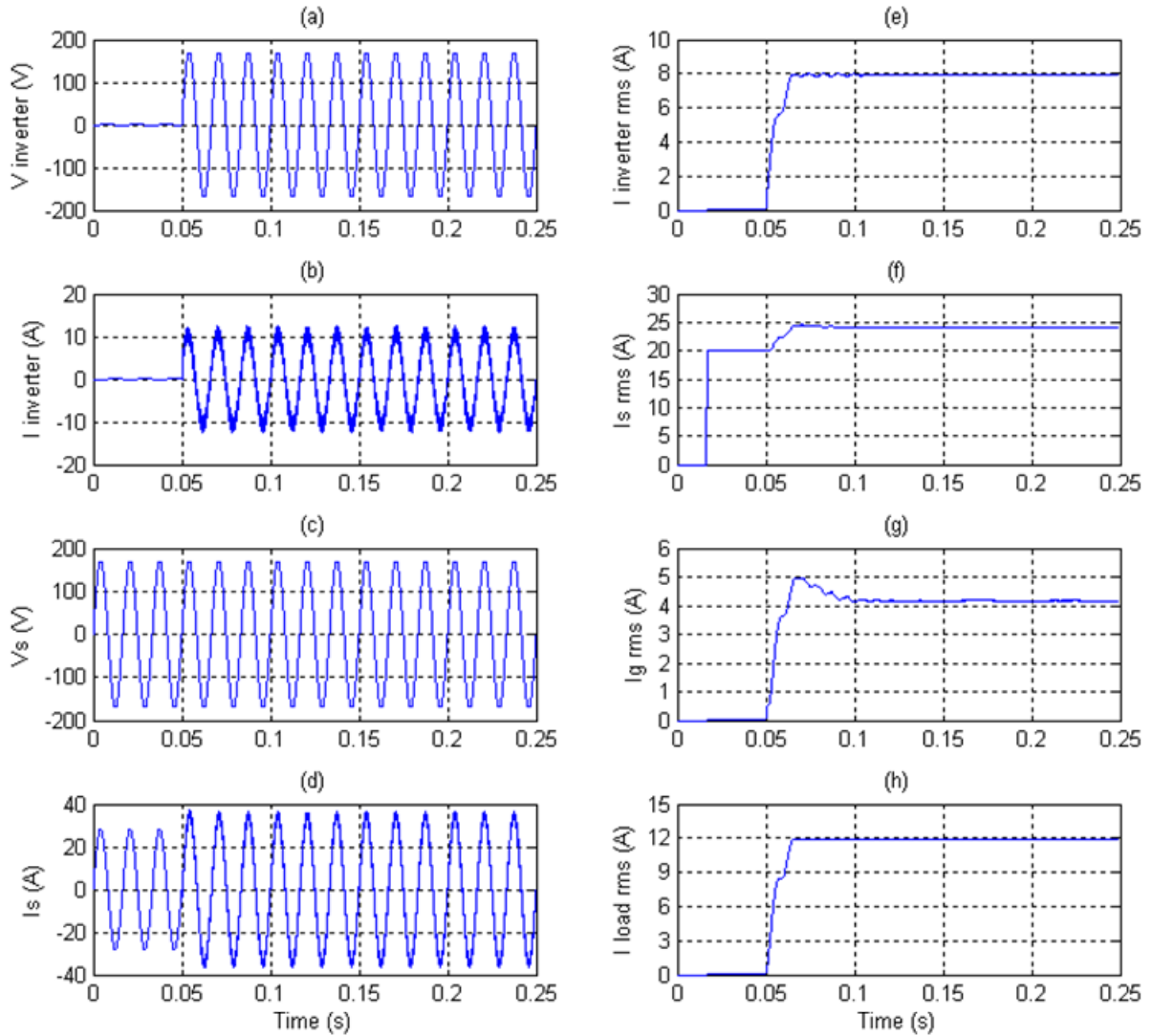


Figure 4. Simulation Results for Current Control Mode of Operation

When the utility breaker is opened, the inverter switches to islanded operation to supply power to the local load. The simulation shows that the utility keeps supplying the utility load but there is no power flowing through the PCC. In the islanded mode of operation, the inverter is voltage controlled to maintain 120V AC, 60Hz voltage for the local load. The voltage and current waveforms in this mode of operation are shown in Figures 5 (a)-(f). From Figure 5 (b), we see that the inverter is maintaining 120V AC rms and supplying current to the local load. The utility voltage and current waveforms are shown in Figures 5 (e)-(f) and it is evident that the utility is supplying power to the utility load.

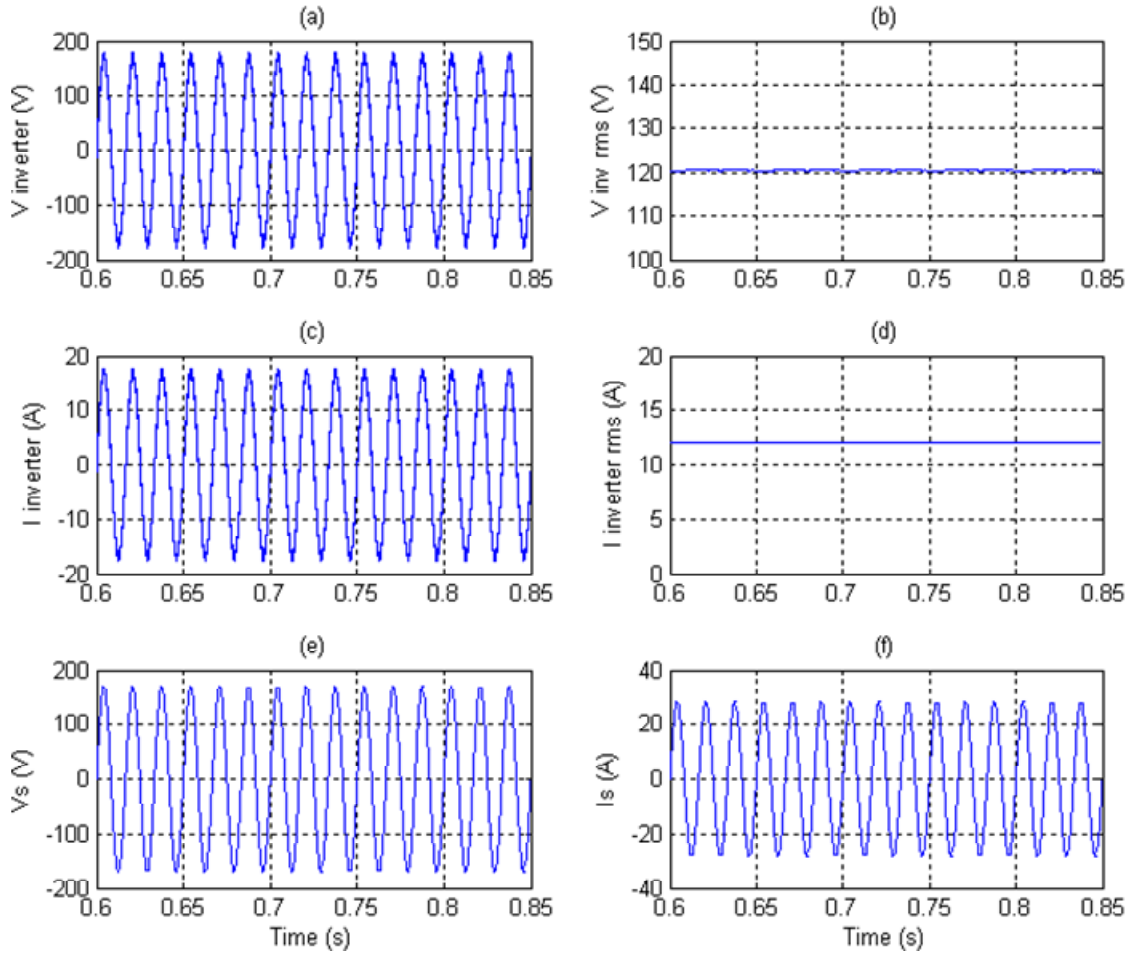


Figure 5. Simulation Results for Voltage Control Mode of Operation

Finally, in Figure 6, we show the voltage and current waveforms from the complete simulation sequence of operation. From these waveforms, we see that the simulated transients during the change in mode of operation from current to voltage control are small. The local load does not experience any variation in voltage (Figure 6 (e)), when the inverter is disconnected from the utility. Also from Figure 6 (d), it is evident that the power is transferring through the PCC only when the inverter is utility connected. From the inverter current waveform, as in Figure 6 (b), we see that the transition from utility-connected to islanded mode is smooth. In the utility-connected mode, the inverter is supplying 8A rms current which is increased to 12A rms when the inverter is in islanded mode supplying the local load.

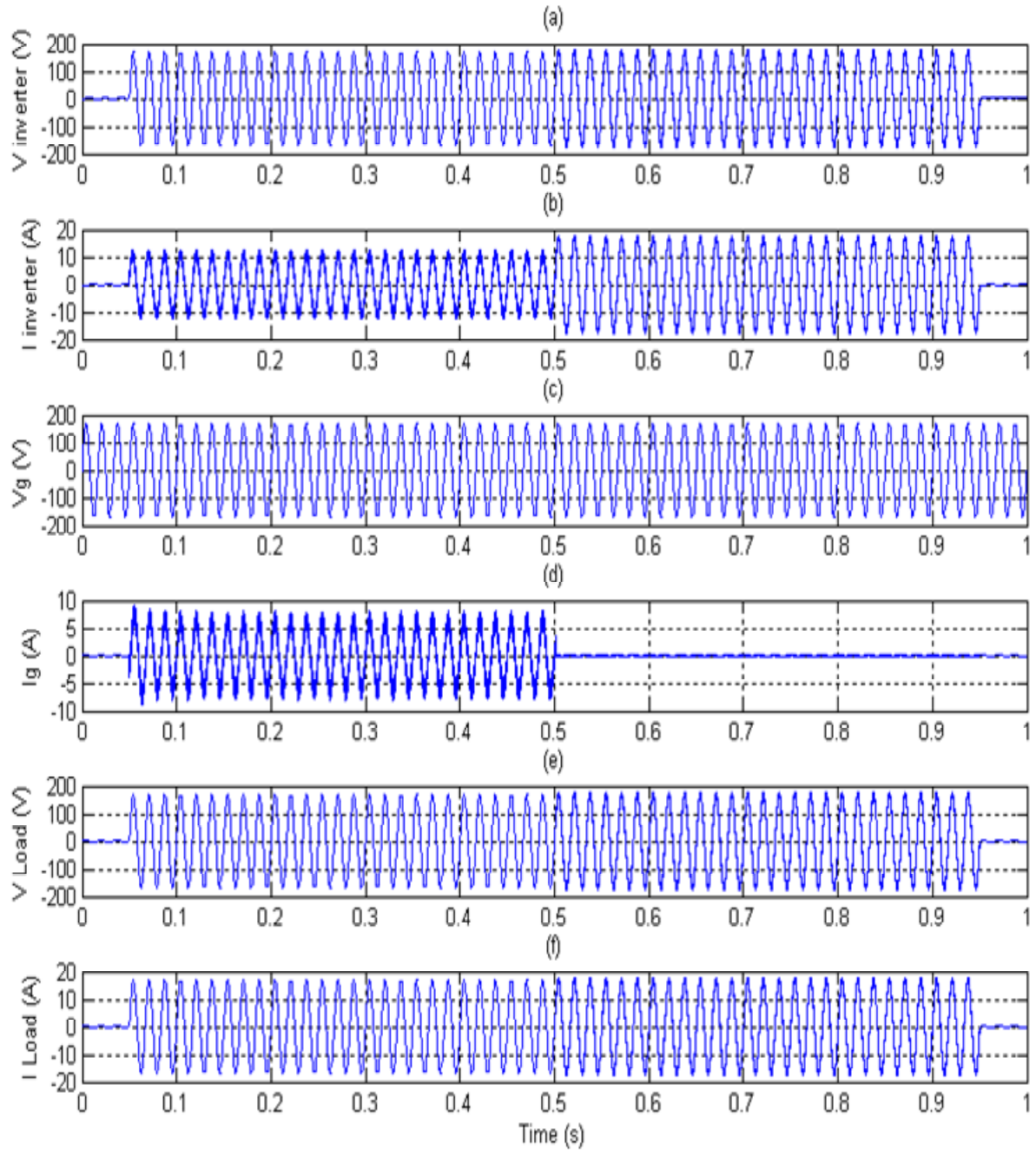


Figure 6. Simulation Waveforms for Complete Inverter Operation

It is important to note that, in Figures 4 to 6, only some representative results are shown based on particular load settings and set points. The inverter model was tested with a variety of different types of loads and different voltage and current reference settings to verify its operation under various scenarios.

3.3 Power Flow Control

The current IEEE Std. 1547 states that the DE system shall not actively regulate the voltage at the PCC, although a utility could allow this mode of operation (Institute 2003). For this reason, most of the commercially available inverters for distributed energy systems operate at unity power factor and do not regulate the local voltage. This can be a concern, because when an inverter only supplies real power, the power factor at the PCC will go down when connected to a lagging power system. Therefore, it would be beneficial for the electric power system if the DE systems could also supply reactive power (Kroposki et al. 2006).

We developed a power flow control algorithm that allows the inverter to generate both active power and reactive power based on the corresponding reference power commands during utility-connected operation. The power flow controller was derived from the current controller as discussed in the previous subsections. In the previous subsections, the current reference setpoint was provided by the user. During power flow control mode, the current reference is calculated using an outer power flow control loop. The reference current amplitude and phase were generated from the power references using equations (3) and (4) respectively, where: P_{ref} is the active power reference, Q_{ref} is the reactive power reference, $(V_{inv})_{rms}$ is the rms output voltage, and $|I_{ref}|_{rms}$ and θ_{ref} are the amplitude and phase of the reference current respectively.

$$|I_{ref}|_{rms} = \frac{\sqrt{(P_{ref})^2 + (Q_{ref})^2}}{(V_{inv})_{rms}} \quad (3)$$

$$\theta_{ref} = \tan^{-1}\left(\frac{Q_{ref}}{P_{ref}}\right) \quad (4)$$

The Simulink block diagram of the outer power flow control loop is shown in Figure 7. The discrete PLL is used to find the utility voltage phase angle. Based on the reference current (I_{ref}) generated by this loop, an inner current control loop, as discussed in Section 3.2.2, was used to develop the 10 kHz PWM switching pattern.

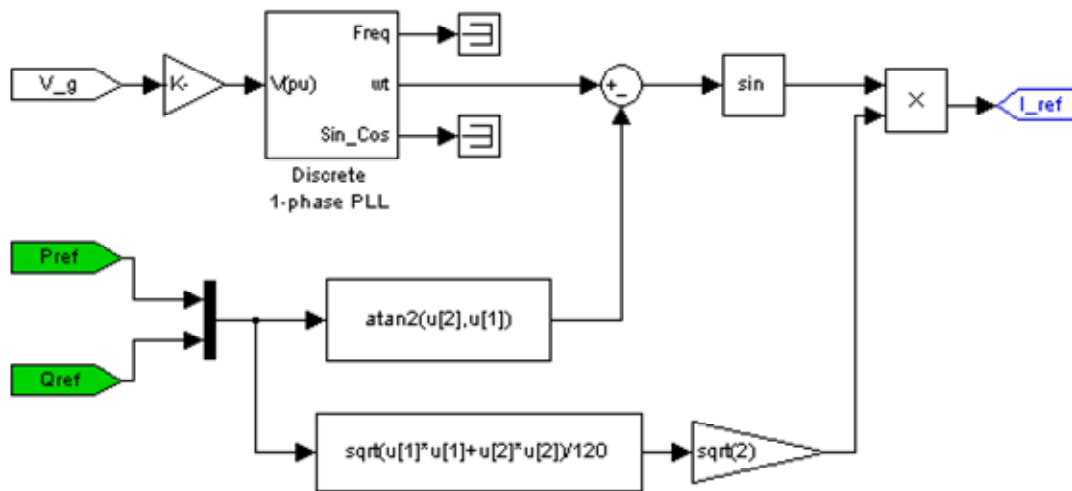


Figure 7. Block Diagram of Power Flow Control Loop

The power circuit shown in Figure 1, was used for simulating power flow control. Again the local load was set as 10Ω resistive and the utility load was set at 6Ω resistive. Active power reference (P_{ref}) was set to $1,000W$ and reactive power reference (Q_{ref}) was set to $1,000 VAR$. According to the convention used, positive reactive power means lagging current.

The simulated power flow waveforms are given in Figures 8 (a)-(h). We see from Figures 8 (a)-(b) that the inverter output powers are following the reference setpoint values. The local load requires $1,440W$; of which $1,000W$ are delivered from the inverter. The remaining active power demand is supplied by the utility through PCC. Since there is no reactive load to compensate for the amount of lagging reactive power generated by the inverter, the simulated utility output generates the same amount of leading reactive power. The results show that the utility is supplying both the utility load ($2400W, 0VAR$) and the remaining local loads are depicted in Figures 8 (c)-(d).

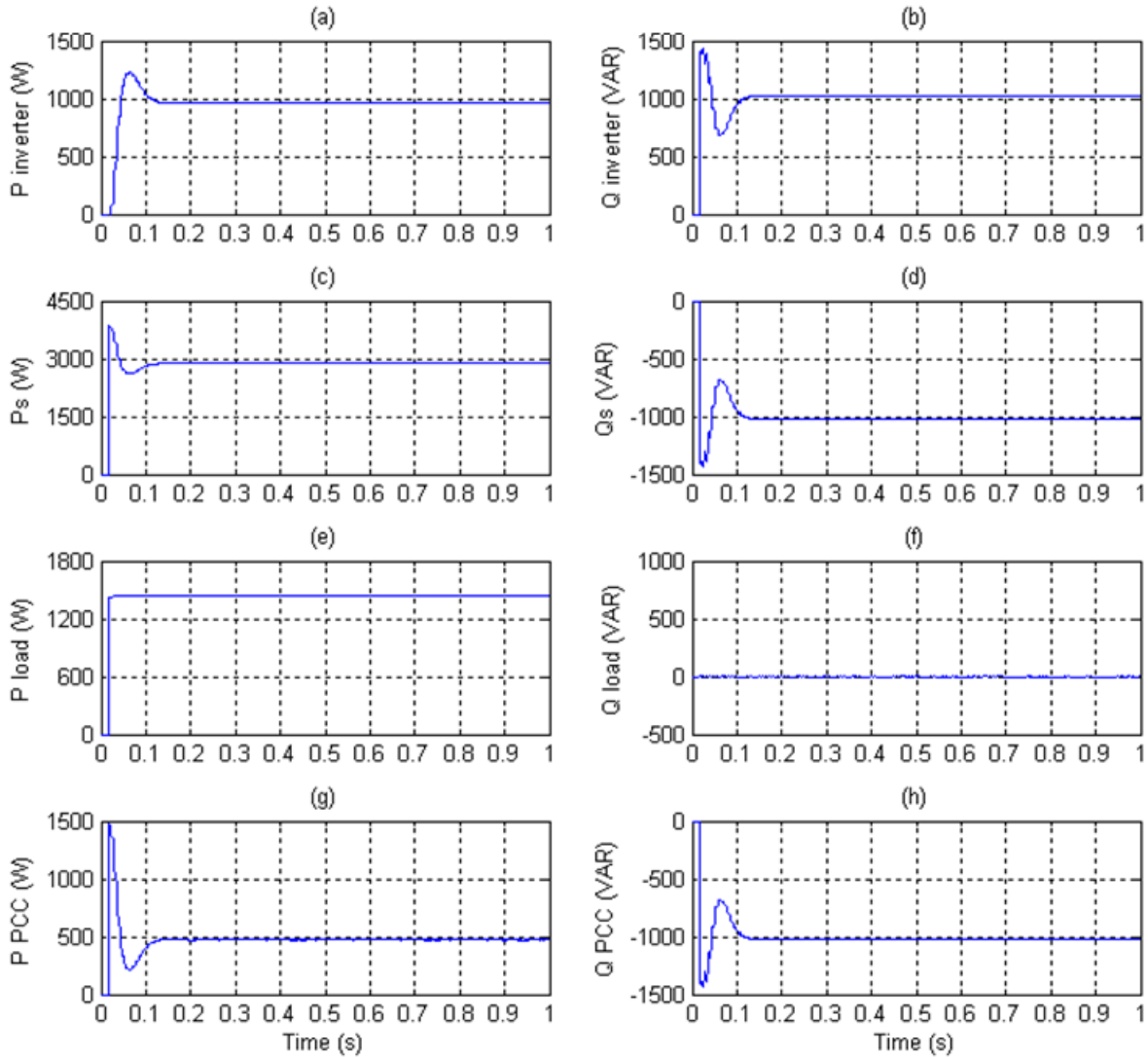


Figure 8. Active and Reactive Power Waveforms for Power Flow Control

The simulated voltage and scaled current waveforms as measured at different parts of the circuit are shown in Figures 9 (a)-(c). As expected, the inverter current is lagging the voltage by approximately 45° (See Figure 9 (a)). The local load voltage and currents are in phase since only resistive loads are present. The utility supplies leading reactive power to compensate for lagging reactive power generated by the inverter; hence the utility current is leading.

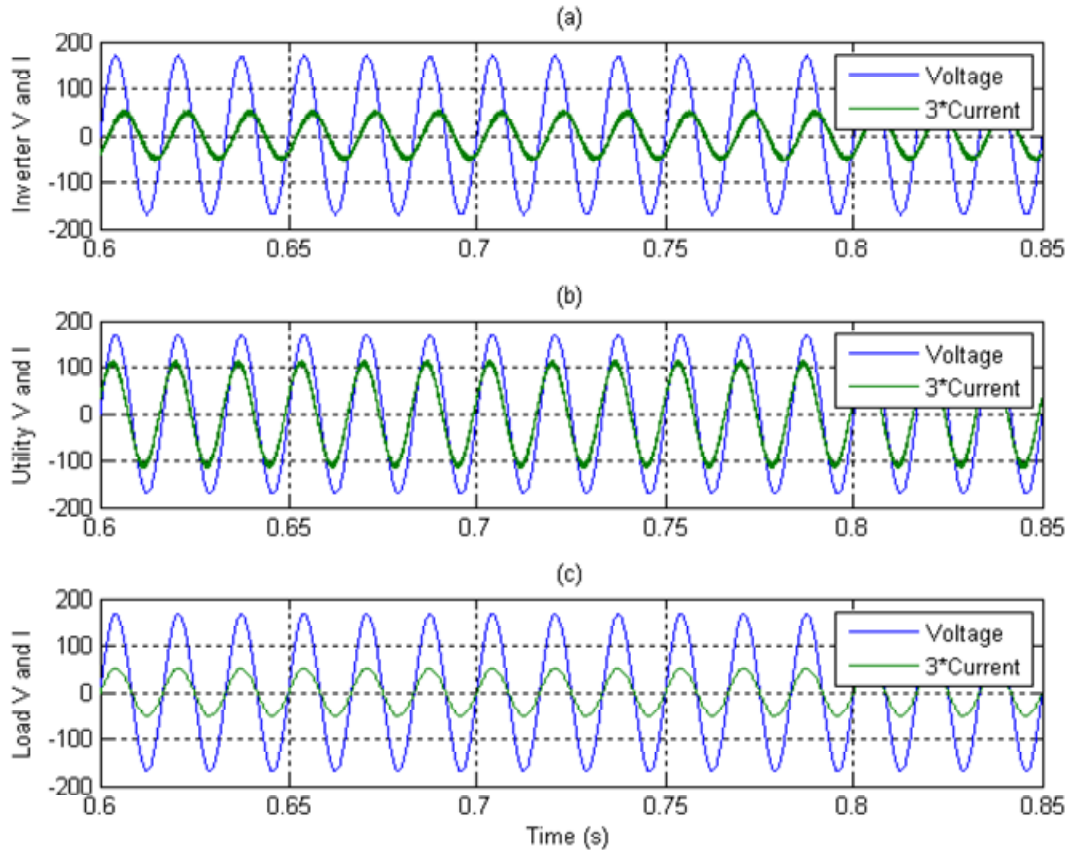


Figure 9. Voltage and Current Waveforms for Power Flow Control

To simulate the response of the power flow control system during step changes in the active and reactive power references, we operated the inverter with a sequence of power commands. At the beginning of the simulation, the inverter was started with $P_{ref} = 1000$ W and $Q_{ref} = -1000$ VAR. At time 0.35s, Q_{ref} was changed through a step function to 1000VAR while P_{ref} was kept constant. Finally, at time 0.7s, a step change in P_{ref} was imposed from 1000W to 600W while Q_{ref} was maintained at 1000VAR.

The simulation results for power flow are shown in Figure 10 (a)-(h). It is evident that the biggest transient occurs during the step change of reactive power from leading VAR to lagging VAR. The transients are mitigated very fast and are damped in less than one cycle. The results show that the inverter output power follows the reference power commands with considerable accuracy.

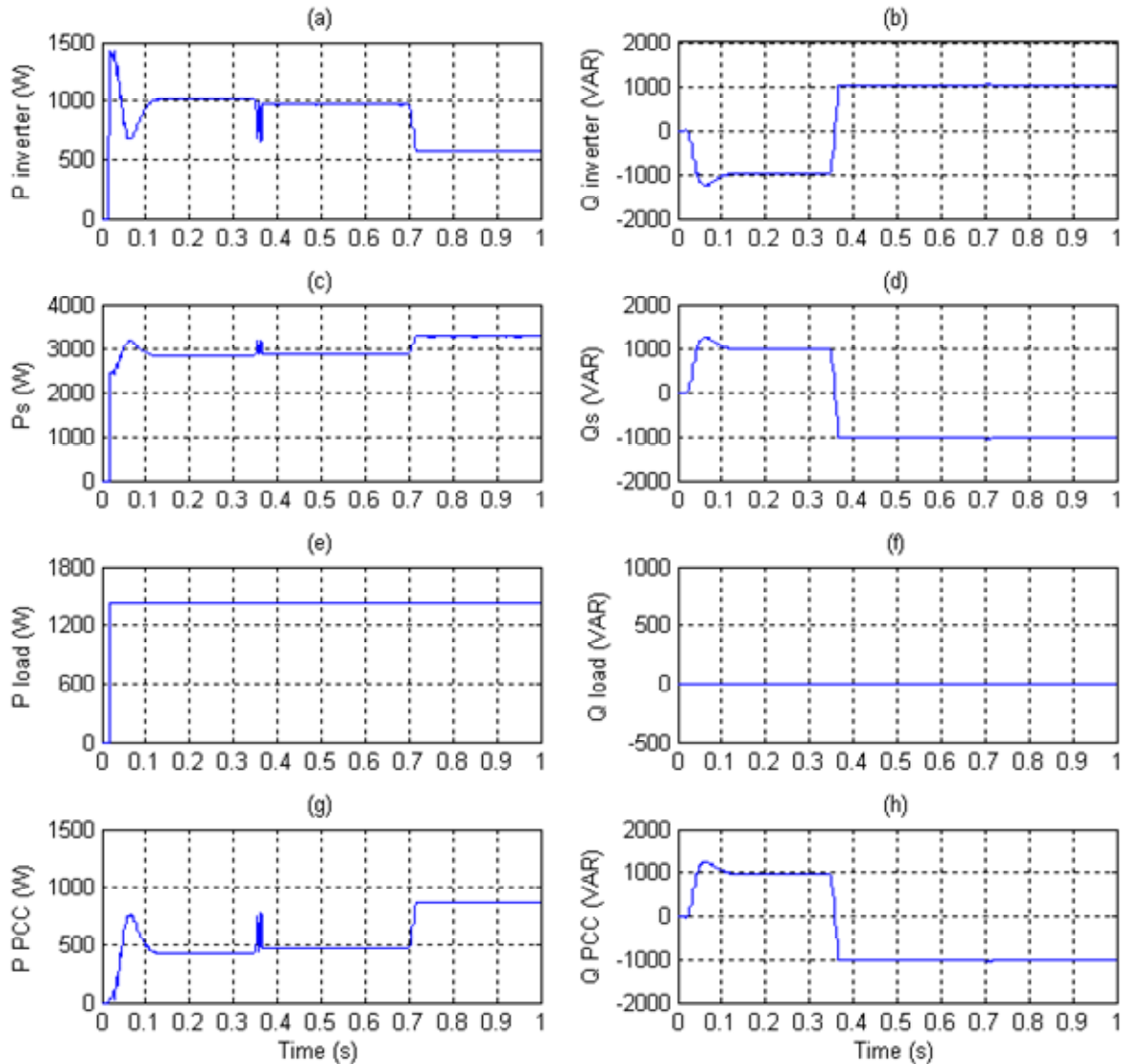


Figure 10. Active and Reactive Power for Step Change in Power Commands

3.4 VAR/Voltage Control

With the improvement of PE, flexible AC transmission systems (FACTS) have opened new prospects for controlling power flow and increasing transmission line capacity (Hingorani and Gyugyi 2000). The PE-based FACTS devices, connected in shunt, can also be used to absorb or generate reactive power; thus controlling voltage profiles in an AC transmission system. The family of FACTS devices without an energy source, which are specifically used for reactive power compensation and voltage regulation, are called static synchronous compensators (STATCOM) (Hingorani and Gyugyi 2000). The voltage-sourced converter scheme for reactive power generation uses a principle that is similar to the conventional rotating synchronous machine. Using a charged capacitor on the DC side, the converter can produce a set of controllable three-phase AC output voltages, which are then coupled to the AC transmission system through small tie reactance. By varying the amplitude of the output

voltage, the reactive power (VAR) flow between STATCOM and the transmission system can be controlled. It is common to use STATCOM only for the reactive power generation and not for the active power by making the output voltage in phase with the AC transmission system voltage. The details of operation and control of STATCOM can be found in (Hingorani and Gyugyi 2000).

The application of STACOM at the distribution voltage level is not very common due to the cost the equipment adds to the system. There are only few papers that discuss implementing distributed-STATCOM (DSTATCOM) at the 11kV AC or higher distribution voltage levels (Twining and Holmes 2003; Rahmati et al. 2006; Mariun et al. 2006). With the increased penetration of DE systems in the utility grid, several studies have been dedicated to finding new markets in forms of ancillary services (Campbell et al. 2005; Barker and DeMello 2000). In these studies, researchers have identified VAR/voltage control as a promising ancillary service that can be obtained from DE systems. Voltage regulation on radial distribution systems is normally maintained using load-tap-changing transformers at substations and/or line voltage regulators or switched capacitors on feeders. It is important to note that IEEE Std. 1547 currently does not allow a DE system to actively regulate the voltage at the PCC, although a utility could allow this mode of operation. But, in the future, if individual DE systems are allowed to regulate VAR, they can also be used to provide voltage support at the low voltage single-phase distribution level (Kroposki et al. 2006).

With increasing penetration of the DE systems in to the electrical distribution network, the DE systems could be equipped with their own PE with the capability of supplying VAR using PE primarily designed for power conversion. This design approach will help utilities to reduce investment into voltage regulation devices. In order for these designs to have large benefits to the utility, the control of the PE equipment must be coordinated with existing equipment on the line.

Simulation Setup

To simulate VAR/voltage control using a single-phase inverter, we modified the power circuit discussed in Section 3.1. The power circuit used for VAR control is shown in Figure 11. In the modified circuit, a series reactance of 13 mH is added to the utility to create a reactive VAR/voltage drop. In the utility-connected mode, depending on the local load settings, the amount of current that flows through this reactance changes and thus can be used for simulating variable VAR drops. This method for testing inverter operation is a simple way to replicate distribution system voltage drop due to VAR requirements and will be helpful for testing the concept in an actual hardware prototype (Section 4).

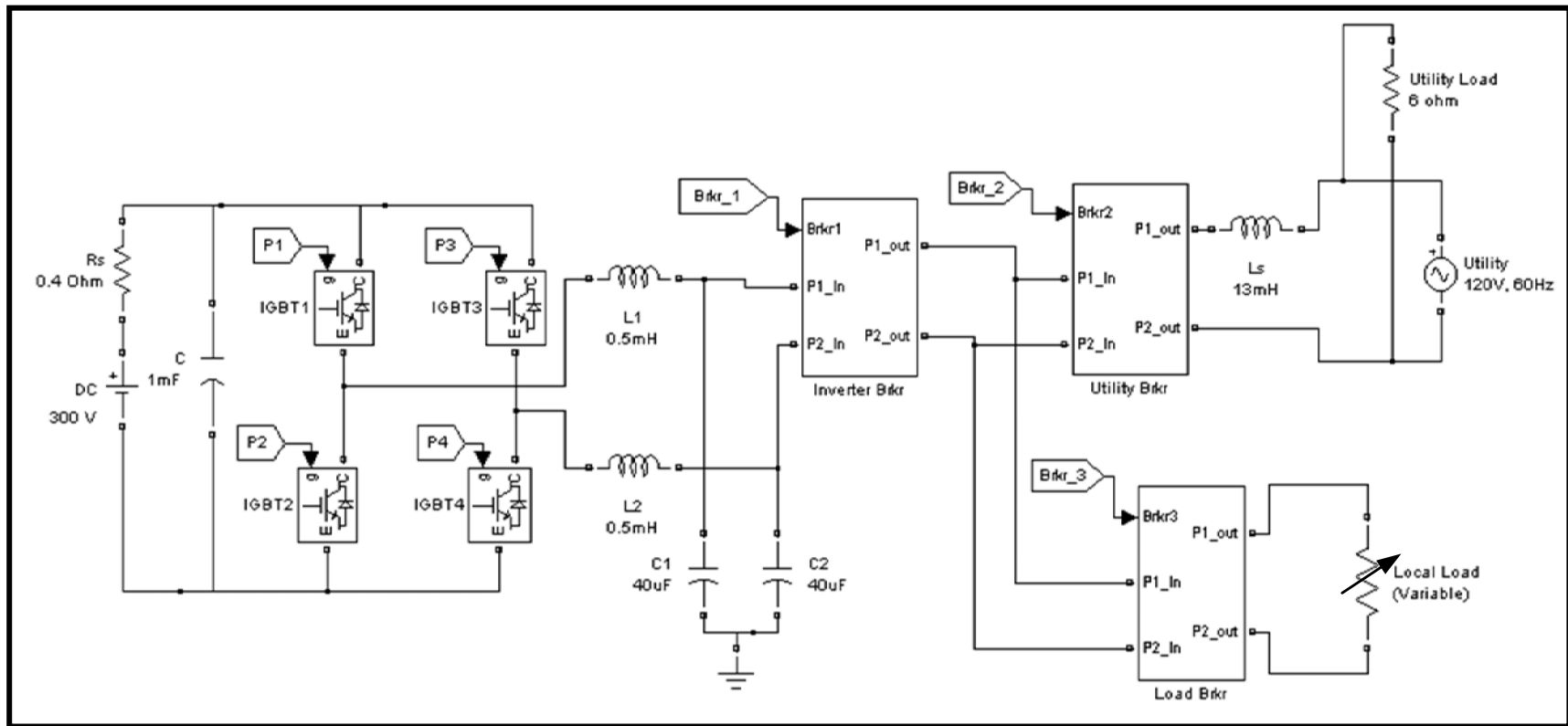


Figure 11. Power Circuit for VAR Control System

The control design for VAR/voltage control has two additional control loops that generate reference active power (P_{ref}) and reference reactive power (Q_{ref}), as shown in Figure 12(a). The reference rms terminal voltage is compared with the actual output rms voltage and is then fed to a proportional controller that outputs Q_{ref} . The DC bus voltage control loop is designed to obtain P_{ref} . The DC voltage loop helps to provide stability for the VAR controller and compensates for converter losses. It should be noted that a DC voltage loop with additional controls could be added to output real power to the distribution system, thus providing power oscillation damping and for leveling peak demand. Although proportional integral (PI) controllers would have given better steady-state results, proportional controllers were chosen for the design to simplify the DSP implementation of the controller.

Based on the power references generated by the VAR control loop, the reference current waveform can be generated as shown in Figure 12(b). Finally, the lower level current controller, as shown in Figure 12(c), uses the reference current waveform to generate 10 kHz PWM switching pattern so that the inverter output current follows the reference current.

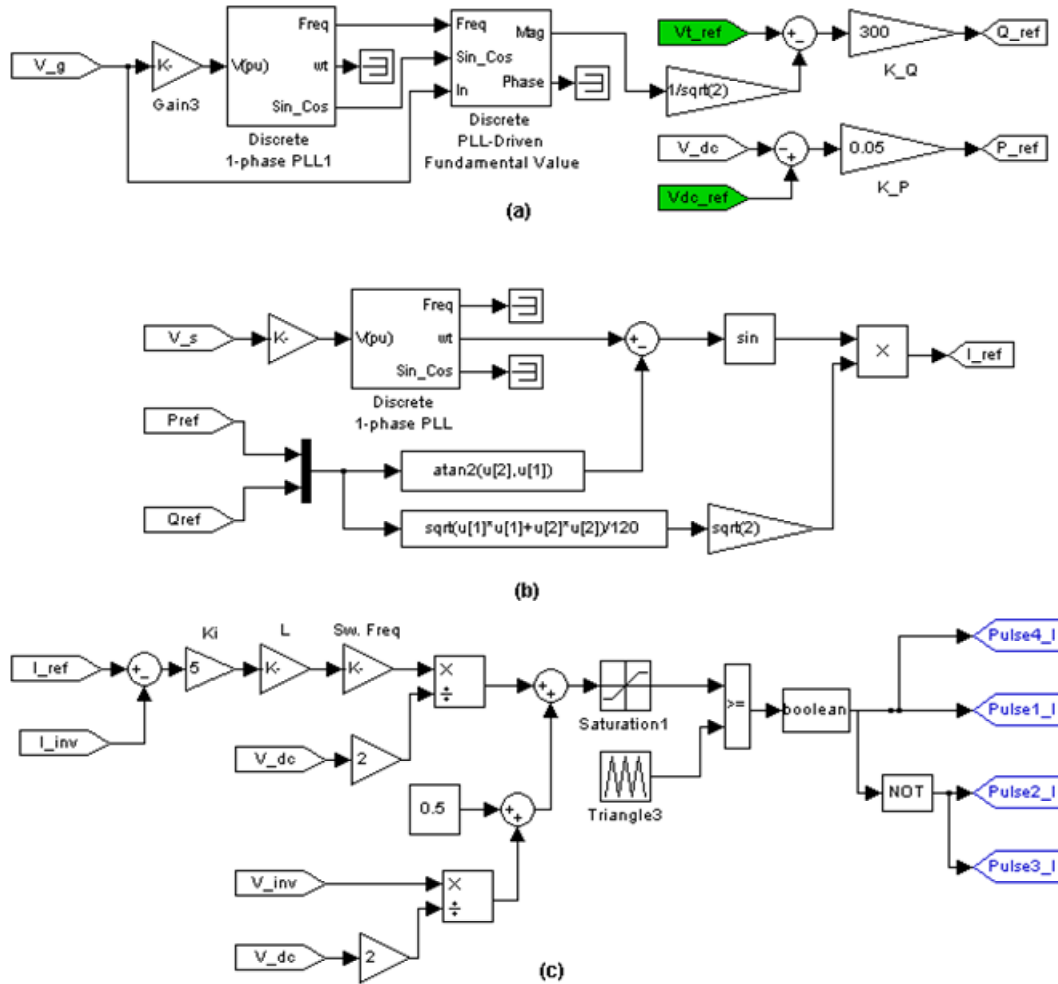


Figure 12. Block Diagram of VAR/Voltage Controller

Simulation Results

In the first case study, the load breaker and utility breaker are closed at time 0.05s; whereas the inverter breaker is left open and the inverter is kept off. At this condition, the utility is supplying both the utility load and the local load. At 0.4s, the inverter contactor is closed and the inverter is turned on in VAR/voltage control mode. During the simulation, the utility load was set at 6Ω and the local load was set at 8Ω .

The voltage waveforms and the corresponding rms values are given in Figures 13 (a)-(f). We can see that when utility is supplying both the load, due to VAR drop at the series reactance, the voltage at the PCC drops to 102V AC rms as shown in Figures 13 (e)-(f). When the inverter is turned on, it starts actively controlling the PCC voltage by supplying VAR. At that condition, the PCC voltage, which is equal to the inverter output voltage, increases to 118V AC rms. A magnified portion of the inverter voltage and scaled current waveforms are shown in Figure 13 (g). As expected, the inverter output current is lagging voltage by 70° . The deviation from 90° is caused by the active power flow through the inverter as shown in Figure 14.

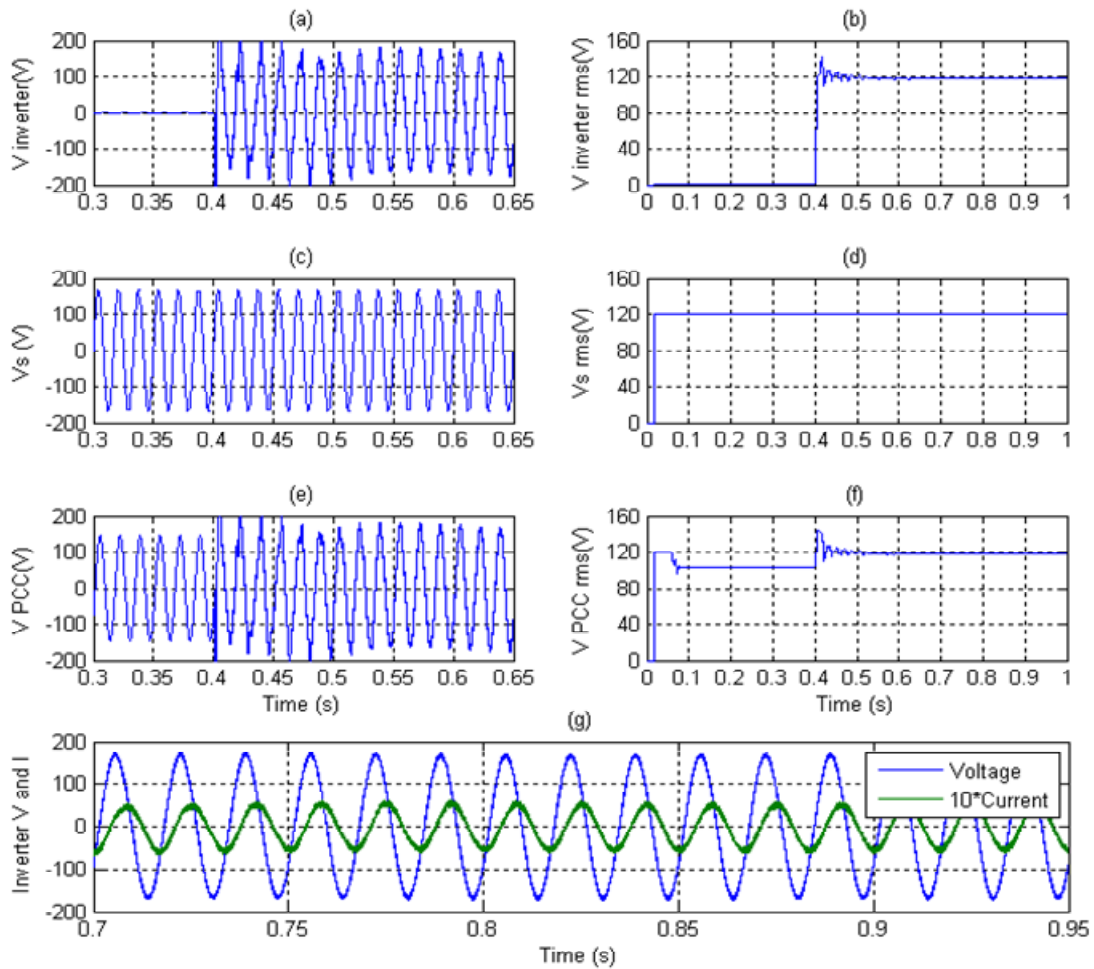


Figure 13. Voltage and Current Waveforms for VAR/Voltage Control

The active and reactive power waveforms are shown in Figures 14 (a)-(f). Before the inverter begins operating, the utility is supplying both the local and utility load equivalent to a total power of about 3,700W. The voltage at PCC is 102V AC rms at this condition; hence the local load requires 1300W which comes from the utility through the PCC to the local load. The utility supplies the reactive power required by the series inductor, which is equal to 800VAR lagging. The local load is resistive, so no VAR needs to be delivered to it. When the inverter is turned on at VAR/voltage control mode, it starts supplying 400 VAR. The reactive power generated by the inverter causes a drop in reactive power required from the utility and therefore improves the voltage at PCC. Under these conditions, the simulated voltage at PCC increases to around 118V AC rms. At this condition, the local load requires 1730W, of which 150W are coming from the inverter and the remaining power is supplied by utility through the PCC. The increase in active power through PCC is due to the fact that at higher voltage, the local load has a higher power demand.

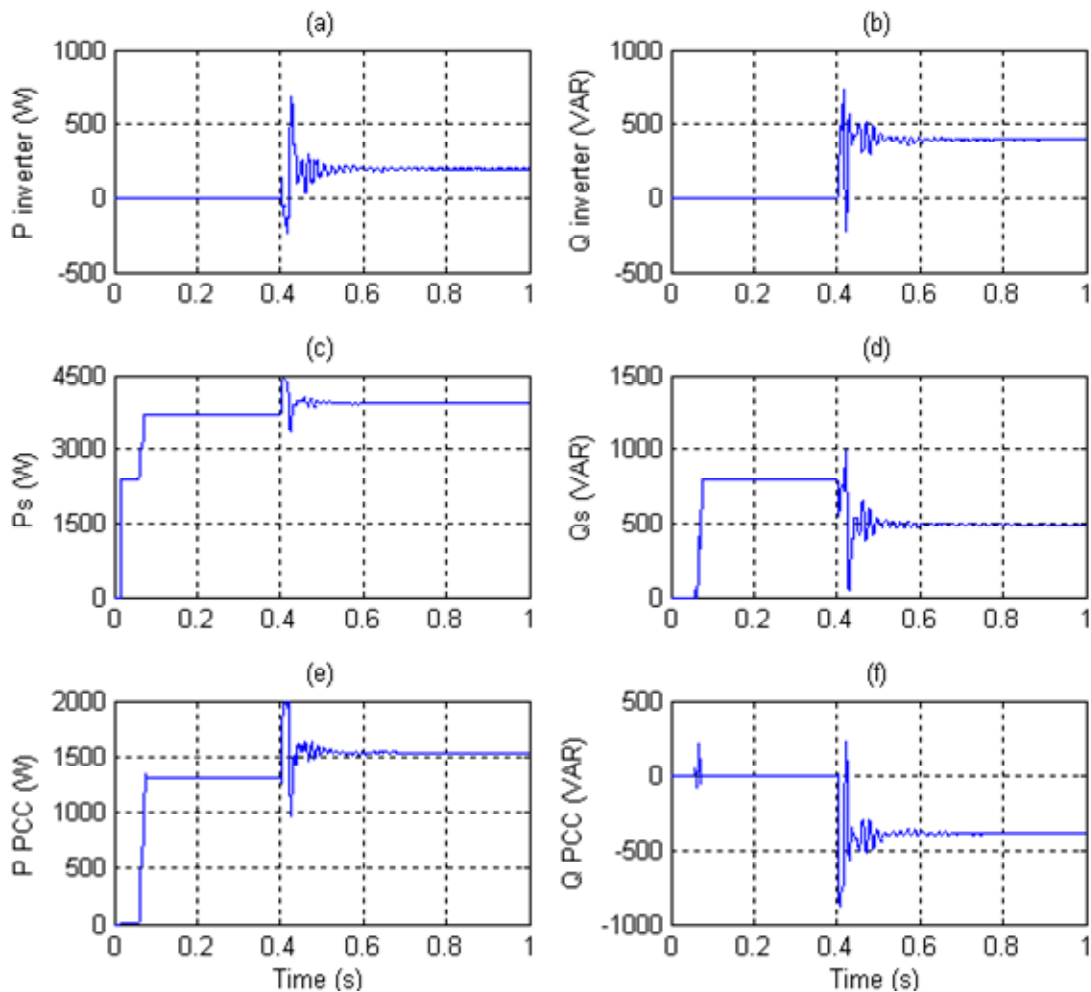


Figure 14. Active and Reactive Power Waveforms for VAR/Voltage Control

In the second case study, we followed a sequence of operation similar to the previous case. The only change in the study was that the local load resistance was set to 15Ω . Since the VAR drop in the series inductor is less, the expected voltage drop will be less. The simulation results are shown in Figure 15 (a)-(f). The voltage at the PCC is 114V AC rms when the inverter is not operating. When the inverter is turned on, it starts supplying 130VAR and improves the PCC voltage to 119V AC rms. This case study confirms that the inverter is capable of supplying varying amounts of VAR to maintain the terminal voltage close to 120V AC rms.

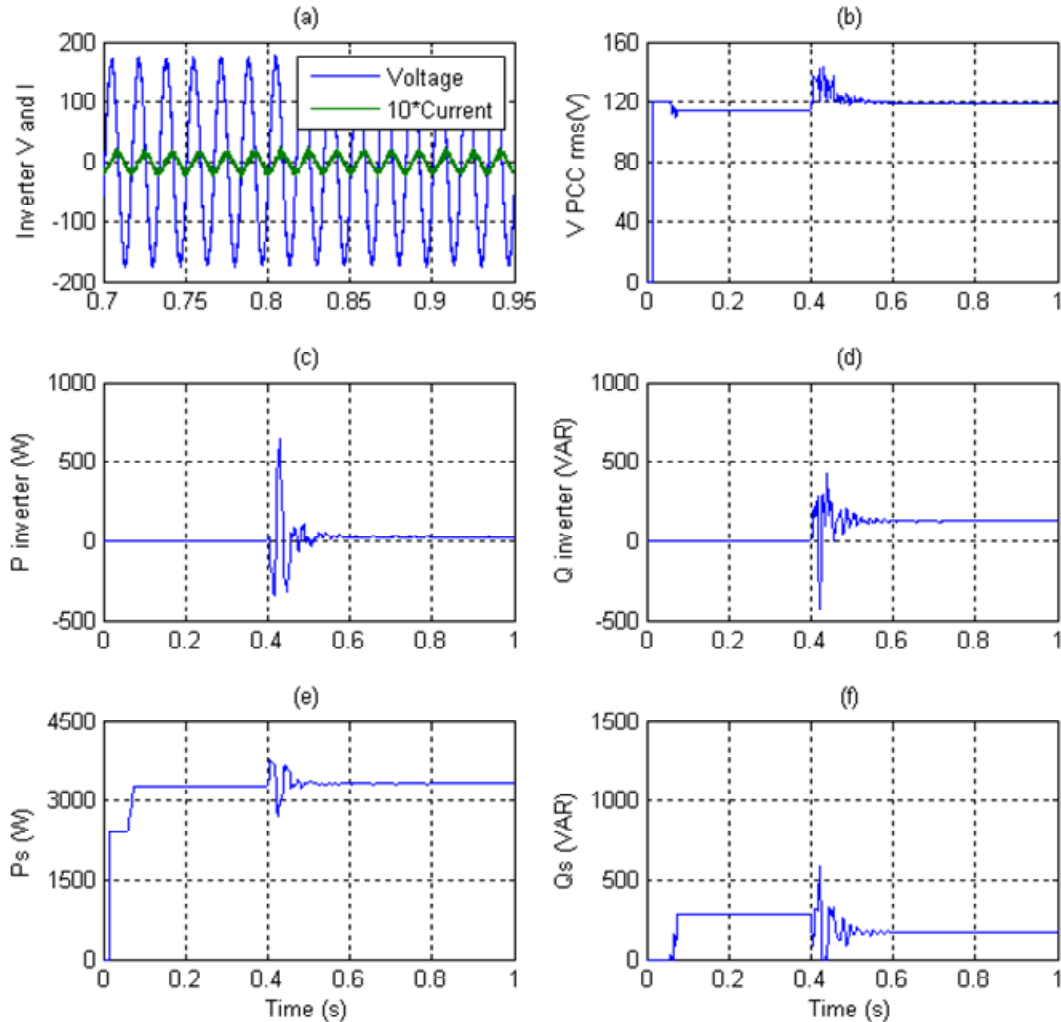


Figure 15. Simulation Waveforms of VAR/Voltage Control for Second Case

4 Hardware Testing

To implement and test new controls such as voltage and VAR regulation, and to increase grid reliability in the transition from grid-tied to islanded operation modes, NREL has built a single-phase inverter hardware platform as detailed in the previous report (Chakraborty et al. 2007). The inverter hardware and controls are designed to ensure modularity and flexibility of the power electronics system. The integrated power electronic modules with IGBTs are used for the power circuit, whereas a DSP-based controller is designed to facilitate the universality of the hardware platform so that it can be used to experiment with different distributed generation sources and/or control objectives.

4.1 Hardware Setup

The laboratory hardware setup consists of several components: inverter power and control circuits, DC voltage source, utility grid simulator, resistive-inductive-capacitive (RLC) load bank, and electronic load bank. The details of the inverter power and control circuits can be found in “Development of Standardized Power Electronic Components, Subsystems, and Systems for Increased Modularity and Scalability” (Chakraborty et al. 2007); a brief description is provided below.

Inverter Power Circuit

In the hardware platform, a SKAI module, manufactured by Semikron USA, was used. The SKAI module consists of six 1200V AC, 300A rms IGBT switches arranged in three-phase bridge format (Semikron). The DC bus filter capacitor, voltage and current sensors, auxiliary power supply, and gate drivers are all included inside the module on a common heat sink. Such integrated modules are often called the integrated power electronics module (IPEM). Though an optional DSP controller can also be included inside the SKAI module, in the laboratory setup an external DSP was selected for this particular design to have more flexibility. The presence of 1 mF capacitance inside the IPEM eliminates the need for external DC bus filters.

Various low DC voltages are required to operate different parts of the hardware. The SKAI module requires 24V DC, the DSP board requires 5V DC, and additional 3.3V DC is required for all the electronic integrated circuits (ICs). A small DC power supply is used for generating 24V DC from 120V AC utility. The 5V DC is developed from the 24V using a buck converter, and a linear regulator circuit is used to develop 3.3V from the 5V. A precision micro-power, low dropout voltage reference IC is used for generating the voltage references for analog-to-digital (A/D) converters in the DSP. Also, level shifters from 3.3V to 5V are utilized to match the control outputs to the SKAI input requirements.

The phase current sensors, DC bus voltage sensor, and heat-sink temperature sensor are integrated in the SKAI module. In addition to those sensors, voltage and current sensors are added to different parts of the hardware to achieve control and protection requirements. Relay circuits are incorporated in to the system in order to facilitate different modes of operations such as utility-connected or islanded operation of the inverter. There are two types of relays used in the setup. The pilot relay contacts are closed by the controller circuit, which are then used to supply the 120V AC to the power relay coils and thus closing the power relays.

The output of the inverter is fed to the LC line filter. The series-connected, 0.5mH inductors and parallel, 40uF capacitors are used to achieve desired voltage and current ripple characteristics.

A picture illustrating the front side of the inverter platform is shown in Figure 16. The detailed circuit diagram for the power circuit and its connection to the control board is shown in Figure 17. The circuit in Figure 17 is for the single-phase inverter where two legs of the three-phase IGBT bridge are used.

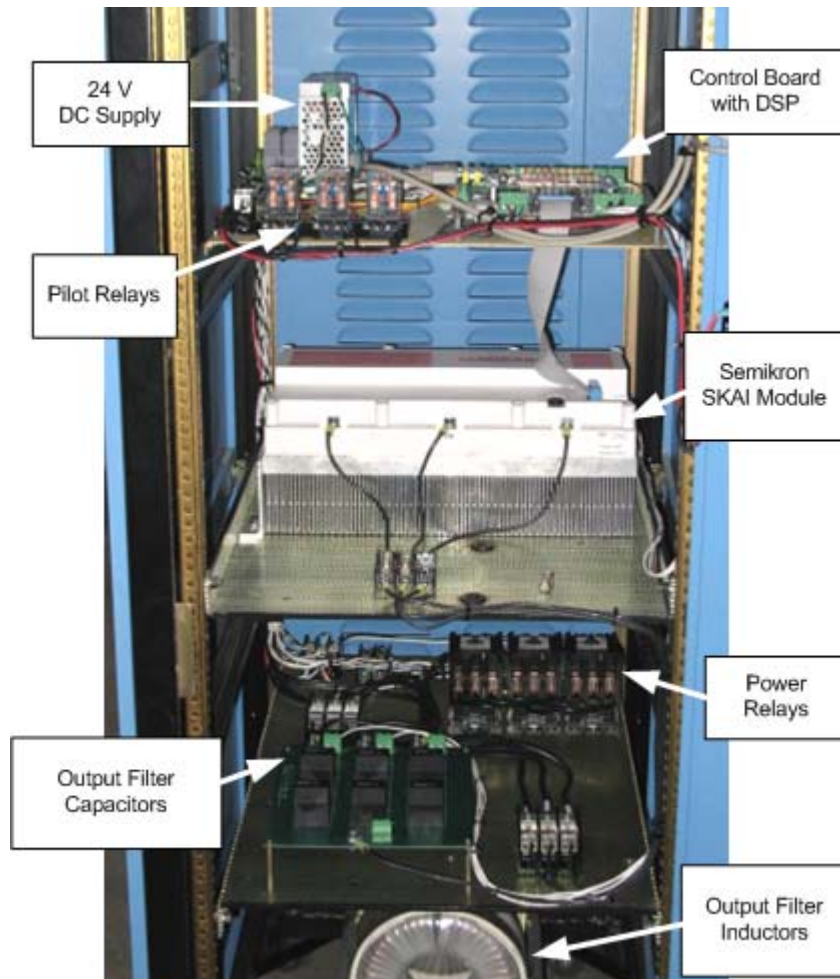


Figure 16. Picture of Front Side of Inverter Platform

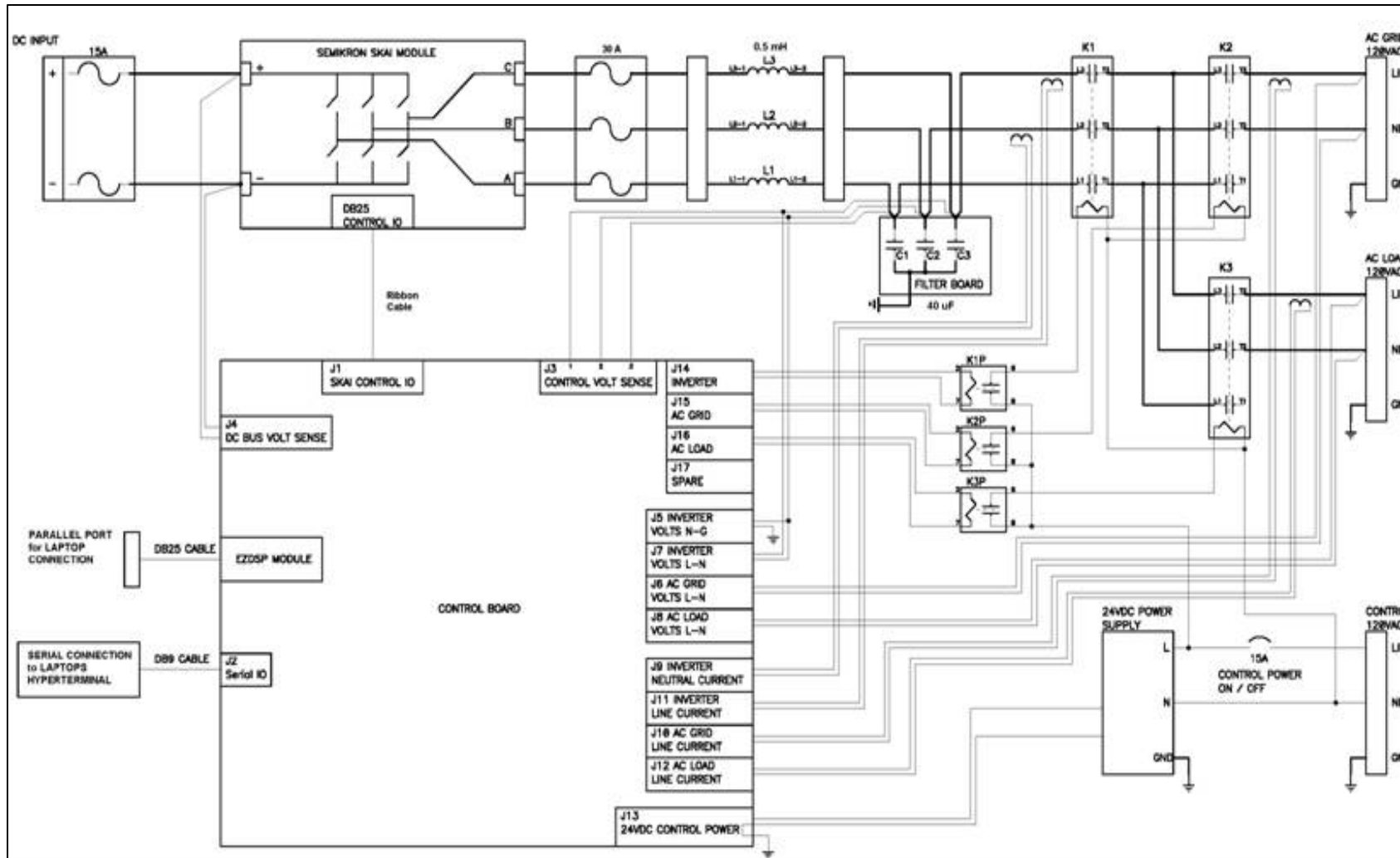


Figure 17. Detailed Power Circuit Diagram and Connections (Drawn in P-CAD)

Inverter Control Circuit

The control board is designed with a Spectrum Digital eZdsp F2812 evaluation module (Spectrum Digital). This module contains the TMS320F2812 DSP by Texas Instruments. To simplify code development and shorten debugging time, a C2000 Tools Code Composer Studio (Texas Instruments) driver is provided with the eZdsp module.

The inputs to the control board are DC bus voltage, phase currents, heat sink temperature, and fault signals from the SKAI module; voltage and current measurement signals from the external sensors; and mode selection and startup signals from the external central processing unit (CPU). The main outputs of the control board are the gate drive PWM signals for the SKAI module. Additionally, the control board also provides enabling signals for the SKAI, PWM status signals to the external CPU, and operating signals for the pilot relays. The local controller is designed to provide control and communication functions for the associated IPEM. As the DSP module has sufficient calculation power, we preferred to carry out all control calculations inside the local controller in addition to the PWM generation for the switches.

The control board has different types of interfaces with the hardware, external human-machine interface (HMI), and external CPU. The power is supplied to the control board by an external AC/DC converter that converts 120V, 60 Hz AC into 24V DC. The signals from the voltage and current sensors are fed directly into the control board, as it has several voltage and current conditioning systems that convert the measured voltage/current into DSP input compatible quantities. The connection between the SKAI module and DSP is obtained using a D-sub 25 pin connector with ribbon cable. The higher level controller in the CPU is currently connected to the DSP board through JTAG-compatible parallel port. An annotated picture of the control board is shown in Figure 18.

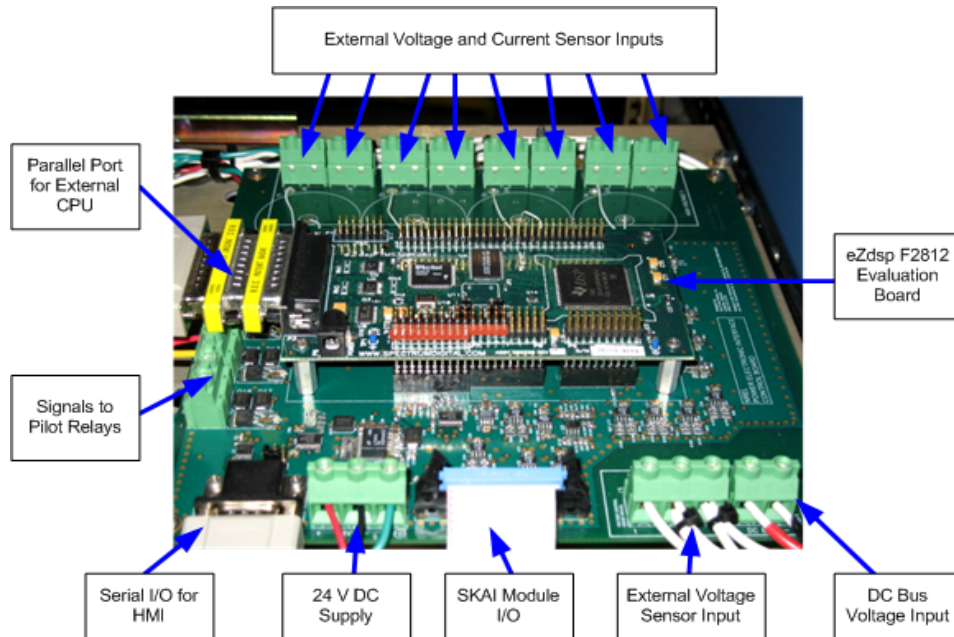


Figure 18. Picture of Control Board with Input/Output Connections

Two methods have been used for DSP code generation. Initially the DSP code was written in C programming language with TI’s Code Composer Studio—all the results that are presented in this section are obtained using these C-based control codes. The C codes were compiled and loaded into the DSP on-chip random access memory (RAM) using Code Composer Studio. Then the controller was activated using the serial interface. The program code is interrupt driven and runs at a fixed sampling frequency of 10 kHz based on the interrupt set up. For the inverter platform, the switching frequency was set at 10 kHz. Therefore, the service routine ran once in each PWM cycle and was used to compute duty cycles for the next cycle. In later stages of the project, the Simulink toolbox was used as a trial to self-generate code; results will be discussed in the next section of the report (Section 5).

Test Setup

In addition to the inverter platform, other components such as DC voltage source, utility grid simulator, RLC load bank, and electronic load bank were connected in the test setup. The DC supply for the inverter was from Xantrex, model no. XDC600-20, with 600V DC, 12kW output. A programmable AC power source, Elgar SmartWave SW 15750, was used as grid simulator (Elgar 2008). The Elgar grid simulator cannot sink power, hence a 200kW RLC controllable load bank, mimicking the utility load, was placed in parallel to the grid simulator. The load terminal of the inverter was connected to a California Instruments 3091LD Series 3kW programmable AC Load. A 1:1 isolation transformer was placed between the inverter output and the grid simulator. The single line diagram of the complete test setup is shown in Figure 19. In addition to the components shown in the figure, for the VAR/voltage control tests, a 13mH air-core inductor was placed between the isolation transformer and the grid simulator. Most of the results, as given in this section, were collected using a Yokogawa PZ4000 Power Analyzer (Yokogawa). Also a Yokogawa DL750 oscilloscope was used, mainly to observe high frequency transients and waveforms.

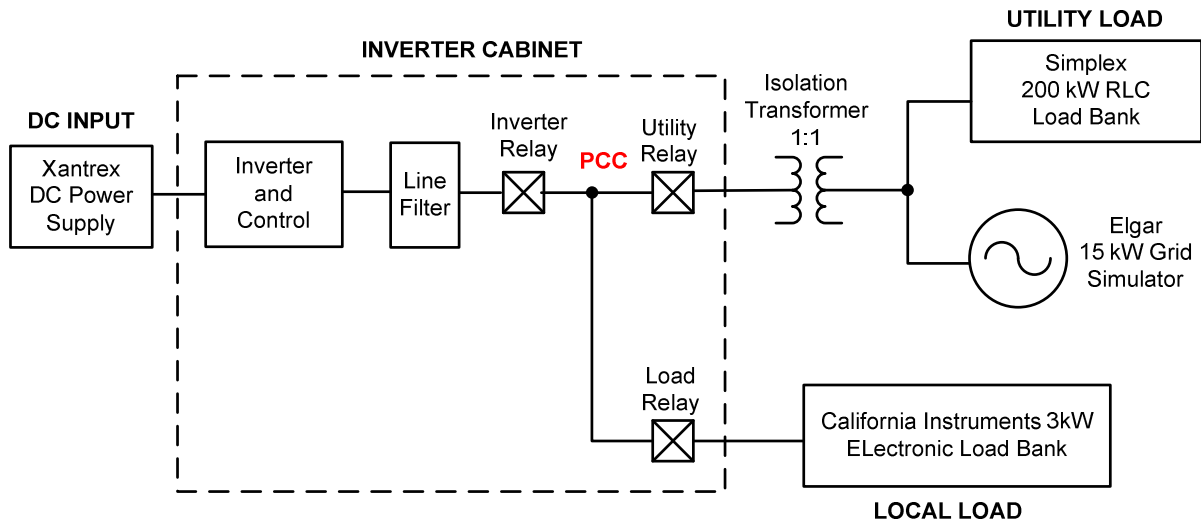


Figure 19. Single Line Diagram of Test Setup

4.2 Experimental Results

The inverter platform was initially evaluated using both islanded-mode voltage control and utility-connected-mode current control. Based on successful operation of the inverter in the current control mode, advanced controllers such as power flow controller and VAR/voltage controller were then implemented in the DSP and tested experimentally.

Islanded Voltage Control

In islanded operation, the inverter has to maintain the amplitude and the frequency of the voltage so that the connected local loads are not affected by utility interruption. The voltage control loop for the inverter is designed for such islanded mode of operation. The control loop is similar to the one developed in SimPowerSystems and shown in Figure 2. But some modifications were implemented in the C-code to obtain better results from the hardware.

When the utility voltage is present, software zero-crossing detection is used to obtain the frequency and phase of the voltage reference, whereas the frequency is set to 60.1 Hz when there is no utility. We have found that the fixed amplitude of the reference voltage causes bigger steady-state errors depending on the change in local load. To overcome this problem, a slower control loop (running at 1/60 s) was designed that changes the amplitude of the reference voltage depending on the output current. After obtaining the reference voltage waveform we designed a voltage controller similar to Figure 2. The final output of the controller is a duty cycle value (D), is given by (5).

$$D = \left(0.5 + \frac{V_{ref}}{2 * V_{dc}} \right) + \frac{K_v * (V_{ref} - V_{inv})}{2 * V_{dc}} \quad (5)$$

where, V_{ref} is the reference voltage, V_{inv} is the inverter output voltage, V_{dc} is the input DC voltage, and K_v is the proportional gain.

The voltage controller operated at each sampling period (set at 10 kHz) and the duty cycle values were updated based on the controller output. The calculated duty cycle value was then limited between 5% and 95% and used to generate a 10 kHz PWM switching pattern. Based on the PWM pattern, the SKAI-module IGBT switches were gated in the bipolar fashion, such that two diagonally opposite switches in the H-bridge turned on/off simultaneously. The DC input voltage was set at 300V DC.

The power analyzer screenshot of experimental results for the voltage control is given in Figure 20. In the figure, channels 1 and 2 show the grid voltage and current respectively. The inverter output voltage and current are displayed in channels 3 and 4 respectively. The utility load is set at 6Ω and the local load is set at 12Ω. The utility is supplying the utility load whereas the inverter is supplying the local loads. The inverter is islanded from the utility and no connection exists between the inverter and the utility as the utility relay is kept open. We can see from the waveforms that the harmonics present in the inverter voltage are low and the inverter voltage is in phase with the utility voltage. Also in the figure, the measurement values for the scope channels are given, where the first column denotes utility quantities and the second column denotes the inverter quantities.

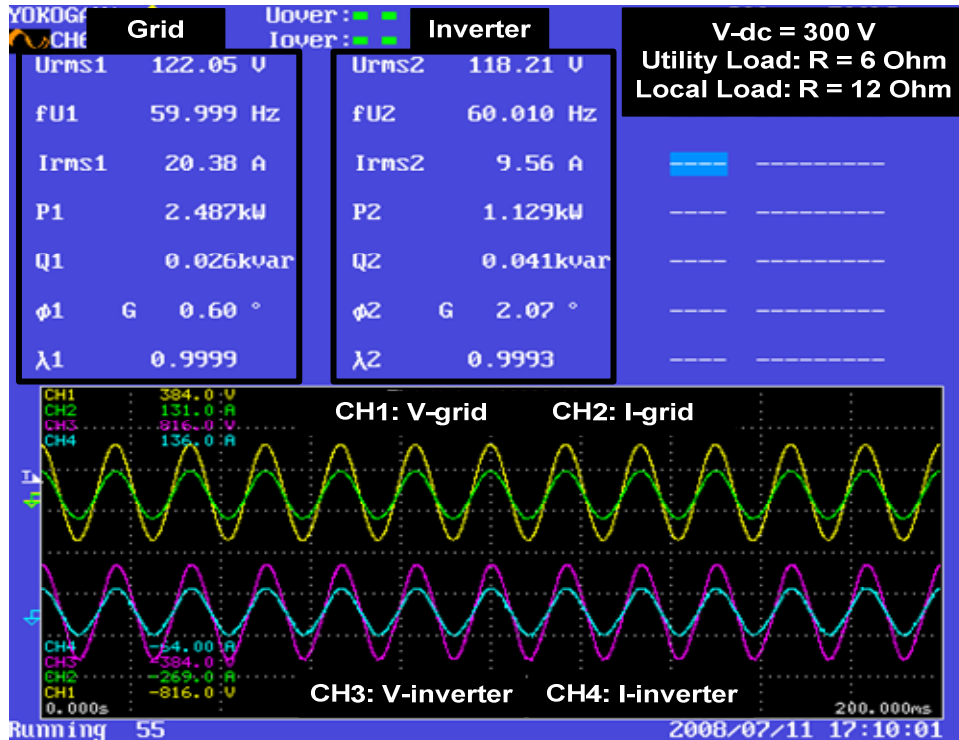


Figure 20. Inverter Voltage Control Experiment

The inverter in the voltage controlled mode was also run for different local loads. The maximum load for the inverter is limited to 20A rms by the measurement and protection circuits. Therefore the local loads were adjusted in such a way that the maximum inverter output current did not exceed 15A rms. The inverter voltage regulation with respect to the output power is shown in Figure 21. The red lines denote the acceptable upper and lower voltage limits as mentioned by ANSI C84.1 (National 1985). We can see that the inverter remains well within the prescribed voltage limit for light load to heavy load conditions, where 200W represents the light load condition. Typically on distribution systems, the voltage will sag with high loading conditions, but in this case the output of the inverter compensates for the high load conditions by raising output voltage.

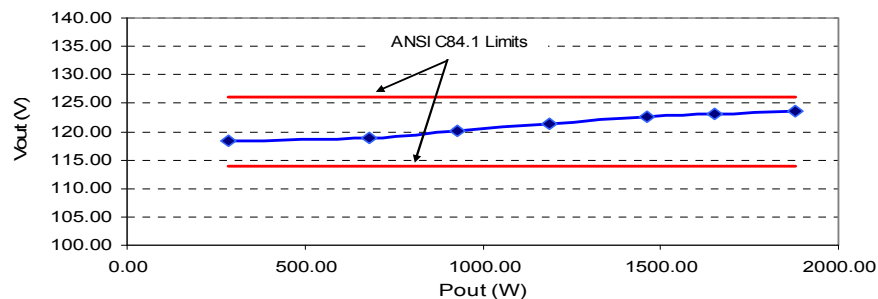


Figure 21. Voltage Regulation of the Voltage-Controlled Inverter

Finally the input-output efficiencies of the inverter are shown in Figure 22 over varying load conditions. It is evident from the figure that the lowest efficiency of 86% occurs at the light load condition and, as loading increases, efficiency also increases. The range of efficiencies

are good considering the fact that the inverter is operating at much lower power levels than the full load of the IGBTs, which are rated for 300A continuous current and 1200V AC rms. Also the inverter platform is built to have some flexibility so that different distributed energy sources can be connected to it in future. The obvious tradeoff to ensure flexibility is that the system and components are underutilized; especially the output LC filters, which are not optimized due to generalized design.

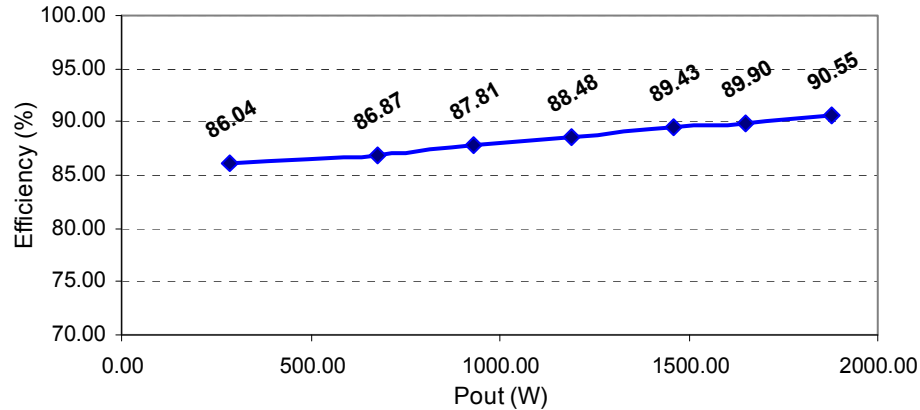


Figure 22. Efficiencies of the Voltage-Controlled Inverter

Utility-Connected Current Control

When the inverter is connected to the utility, the grid controls the amplitude and frequency of the inverter output voltage, and the inverter itself operates in the current control mode. The currents required by both the local load and the utility load are shared by the inverter and the utility, where the inverter provides the amount of current based on the reference current.

In the current controller, software zero-crossing detection was used to obtain the frequency and phase of the utility voltage, which was then used along with the user-defined phase angle and current amplitude to calculate the reference current waveform. After obtaining the reference current waveform the current controller (similar to Figure 3) was designed. The final output of the current controller is a duty cycle value (D), as given by (6).

$$D = \left(0.5 + \frac{V_{inv}}{2 * V_{dc}} \right) + \frac{K_i * (I_{ref} - I_{inv}) * L * f_{sw}}{V_{dc}} \quad (6)$$

where, V_{inv} is the inverter output voltage, V_{dc} is the input DC voltage, I_{ref} is the reference current, I_{inv} is the inverter output current, K_i is the proportional gain, L is the gain equal to filter inductance of $500e-6$, and f_{sw} is the gain equal to switching frequency 10,000.

The PWM generation is the same as described in the voltage controller section. Based on the PWM pattern, the SKAI module IGBT switches were gated in a bipolar fashion, such that two diagonally opposite switches in the H-bridge turned on/off simultaneously. The DC input voltage was set at 300V DC.

The current control loop was tested with different amplitude and phase reference values. A screenshot from the power analyzer is given in Figure 23. In the figure, the red curve indicates utility voltage, the purple curve indicates inverter voltage, and the light blue curve denotes inverter output current. In this case study (case 1), the reference current was set at 8A rms at unity power factor (upf). The utility load is set at 6Ω and the local load is set at 12Ω . Also in the figure, the measurement values for the scope channels are given. It can be observed from the measurements that the inverter is supplying around 8A at upf. The total load demand is approximately 30A (20A for utility load and 10A for local load), of which the inverter is supplying 8A and rest is coming from the utility.

Another screenshot from the scope is given in Figure 24. In this case (case 2), the amplitude of the reference current is set at 9A rms and the phase is set at 50° . Again it is evident from the figure that the output current is following the reference current well.

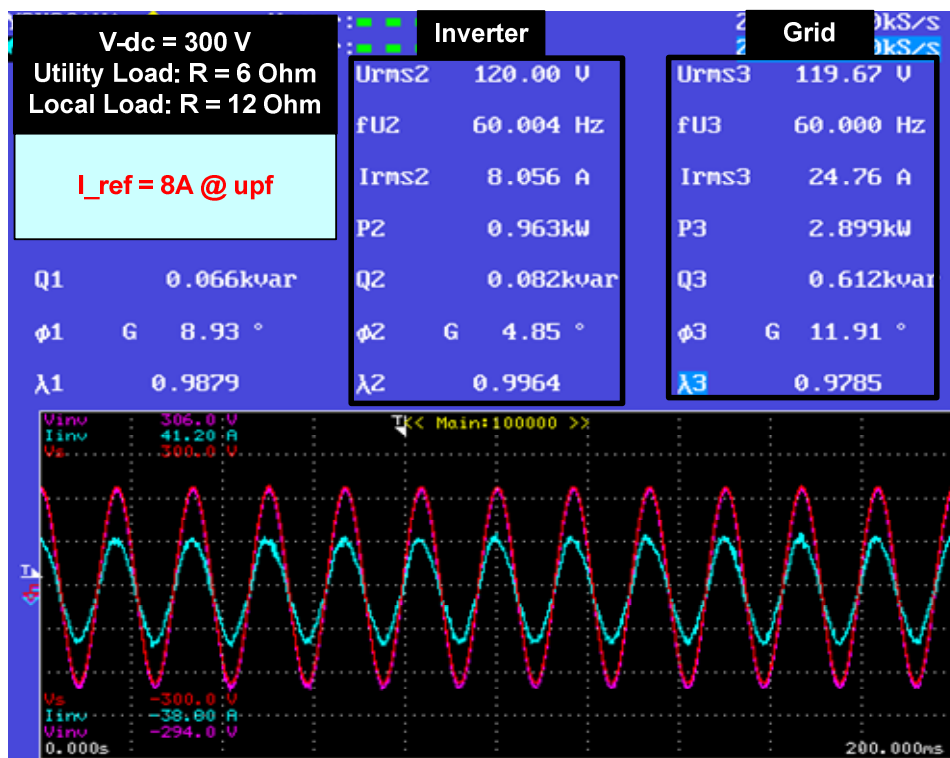


Figure 23. Inverter Current Control (Case 1)

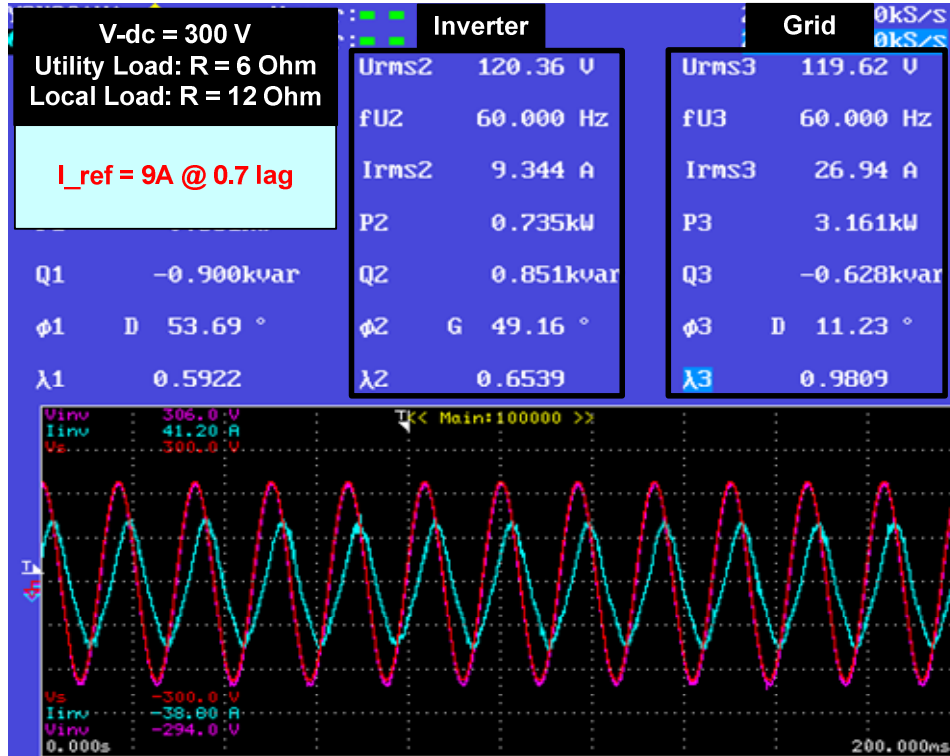
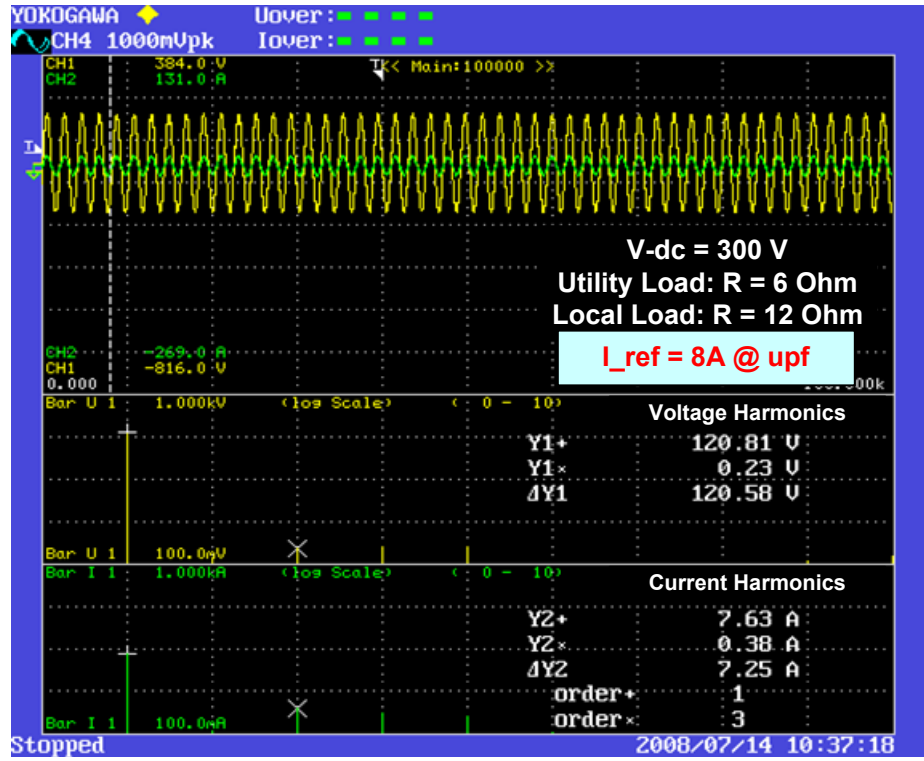
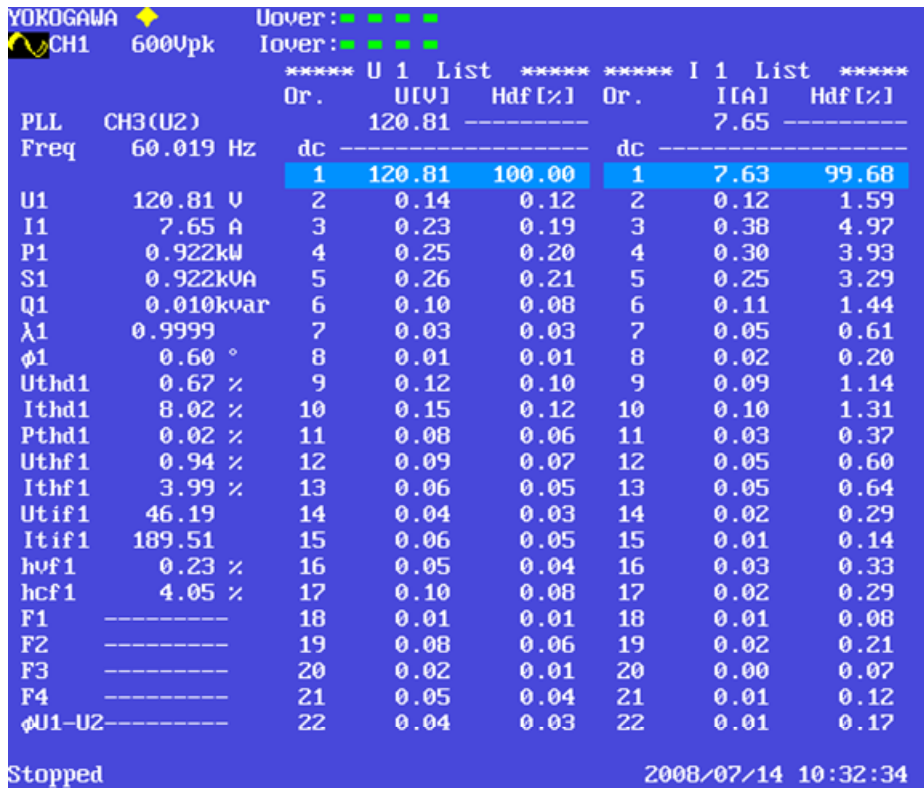


Figure 24. Inverter Current Control (Case 2)

The Yokogawa PZ4000 Power Analyzer was used for harmonic analysis of the voltage and current waveforms for the current-controlled mode of operation. The analysis is based on current control case 1 where the reference current was set at 8A rms at unity power factor. In Figure 25 (a), the inverter voltage and current waveforms are shown in the top axis, followed by frequency spectrum of the voltage and current in the middle and bottom axes respectively. The complete list of calculated variables based on the harmonic analysis is given in Figure 25(b). From this figure, we see that the inverter voltage has very little harmonics content. We expect this because in the utility-connected mode, utility voltage and inverter output voltage are same, coupled through a 1:1 isolation transformer. The total harmonic distortion (THD) of the inverter current is 8%, which is slightly higher than the preferred value of 5% as indicated in the IEEE 1547 interconnection standard (Institute 2003). As mentioned earlier, however, the output line filters and the current transducers used in the hardware setup were not optimized; therefore such harmonic content in the experimental result is expected.



(a)



(b)

Figure 25. Harmonic Analysis by Yokogawa Scope

Finally, as with the voltage control mode, the inverter was run in current control mode with varying current references to obtain the voltage regulation and efficiencies from light load to heavy load conditions. The inverter voltage regulation with respect to the output power is shown in Figure 26. The red lines denote the acceptable upper and lower voltage limits as mentioned by ANSI C84.1 (National 1985). We see that the inverter voltage remains within the prescribed voltage limit with varying load scenarios. The input-output efficiencies of the inverter are shown in Figure 27. From the figure it can be seen that the efficiencies lie in the range of 88%-90% and the trend is similar to that of the voltage control mode.

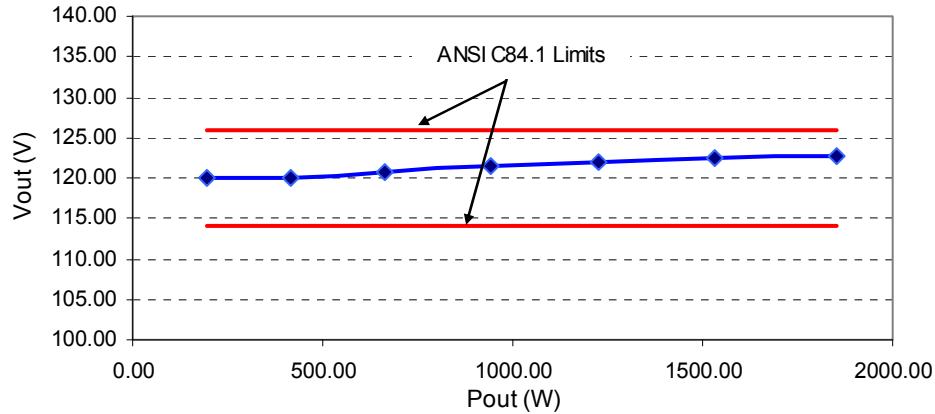


Figure 26. Voltage Regulation of the Current-Controlled Inverter

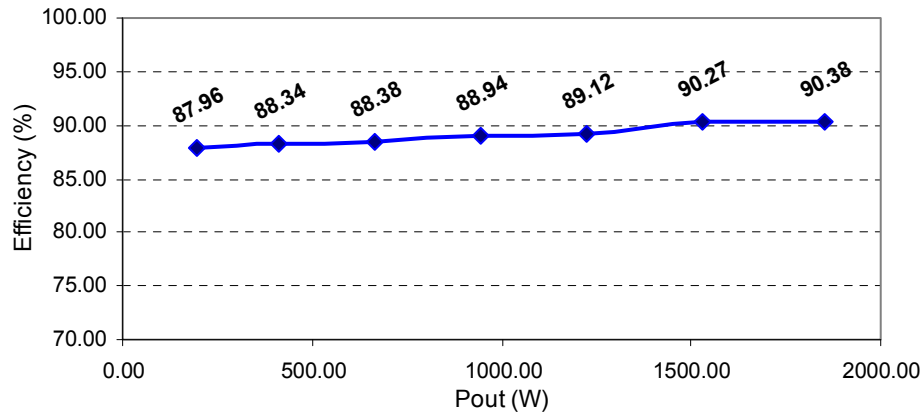


Figure 27. Efficiencies of the Current-Controlled Inverter

Power Flow Control

In the power flow control mode, the inverter operates utility-connected and generates both active and reactive power based on the corresponding reference values. As mentioned in the section on modeling and simulation, the basic design of the power flow controller depends on the lower level current control loop. The amplitude and phase of the reference current waveform is calculated from the active and reactive power references (P_{ref} and Q_{ref} respectively) by the following equations.

$$|I_{ref}|_{rms} = \frac{\sqrt{(P_{ref})^2 + (Q_{ref})^2}}{(V_{inv})_{rms}} \quad (7)$$

$$\theta_{ref} = \tan^{-1}\left(\frac{Q_{ref}}{P_{ref}}\right) \quad (8)$$

Based on the polarity of the reference reactive power, different scaling gains are used on the calculated current amplitude reference to minimize steady-state errors. The power flow calculations are performed in the slower control loop running at 1/60 s; that means the amplitude and the phase values for the current reference are updated once in each voltage cycle. Based on these values, the fast 10 kHz interrupt-driven current controller generates the 10 kHz PWM switching pattern, as discussed in the previous subsection. As with the previous voltage and current controller, the IGBT switches are gated in the bipolar fashion and the DC bus voltage is set at 300V DC. The utility load is set at 6Ω and the local load is set at 12Ω.

The experimental results for the power flow control are shown in Figures 28 to 30. In these figures, channels 1 and 2 show the utility voltage and current respectively. The inverter output voltage and current are displayed in channels 3 and 4 respectively. Also in the figure, the measurement values for the scope channels are given, where the first column denotes utility quantities and the second column denotes the inverter quantities.

The power analyzer screenshot for the case where P_{ref} is set to 1,200W and Q_{ref} is zero is given in Figure 28. We can see from the figure that the inverter output current rms is around 10.56A, which is slightly higher than the expected rms current. Steady-state errors are present for both the active and reactive power outputs; this is expected, as only the proportional controller is used in the system. The output current from the inverter is in phase with the output voltage. In Figure 29, the screenshot shows the case where P_{ref} is zero and Q_{ref} is 1,100VAR. According to the reactive power convention used, positive reactive power indicates lagging current as can be verified by Figure 29. The current is lagging the voltage by approximately 90°. Finally, in Figures 30 (a)-(b), experimental results for the cases when P_{ref} is set at 700W and Q_{ref} is set at 700 and -700VAR are given. From all these case studies, we conclude that the power flow control is working fine with small steady-state errors between the reference power commands and the actual output powers.

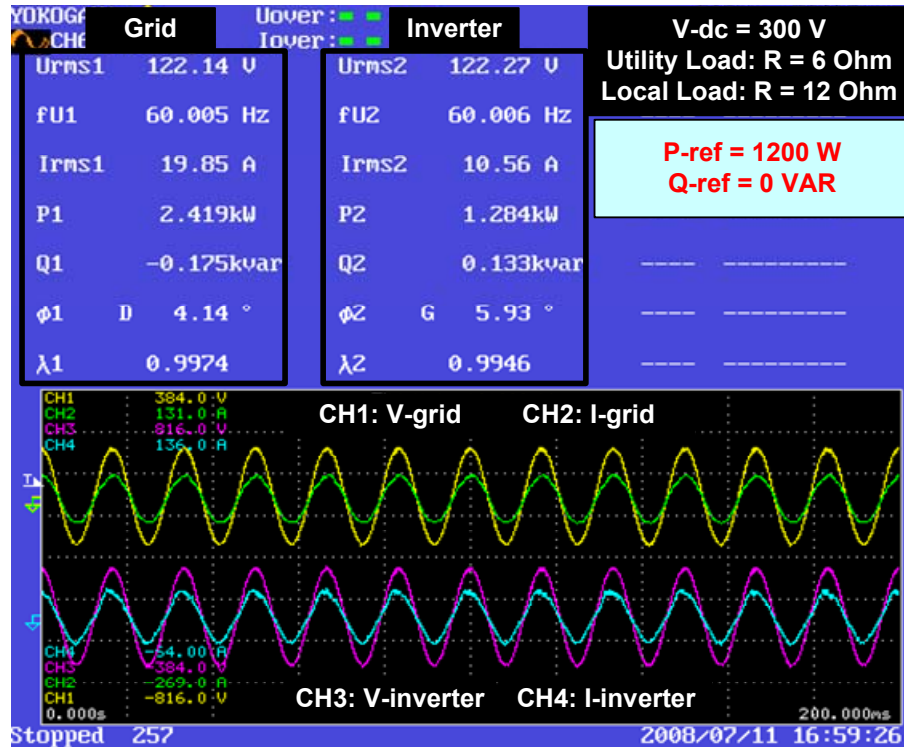


Figure 28. Inverter Power Flow Control (P=1200W, Q=0)

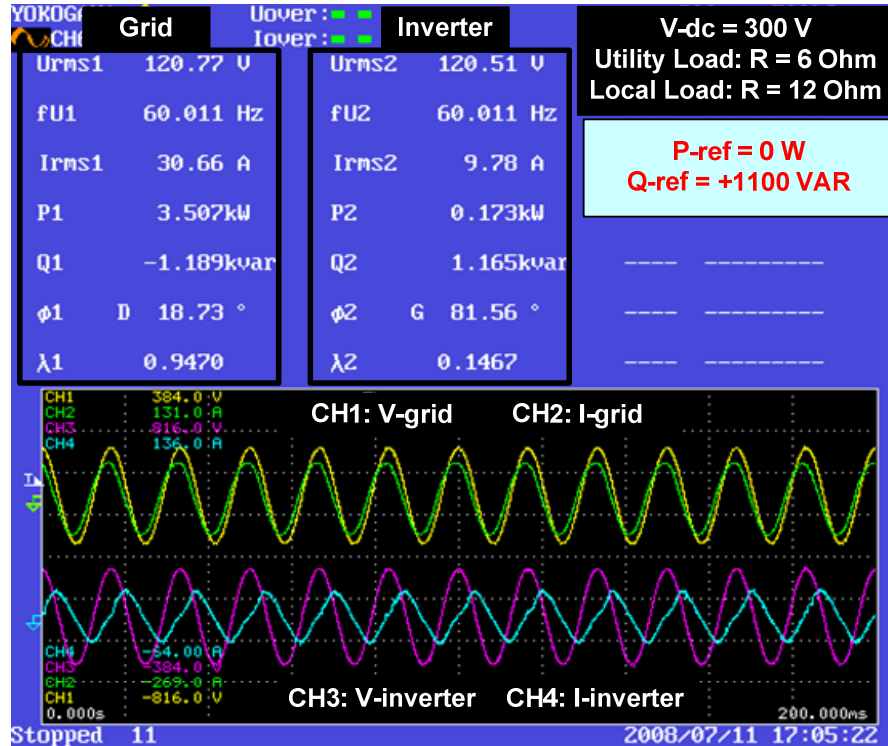
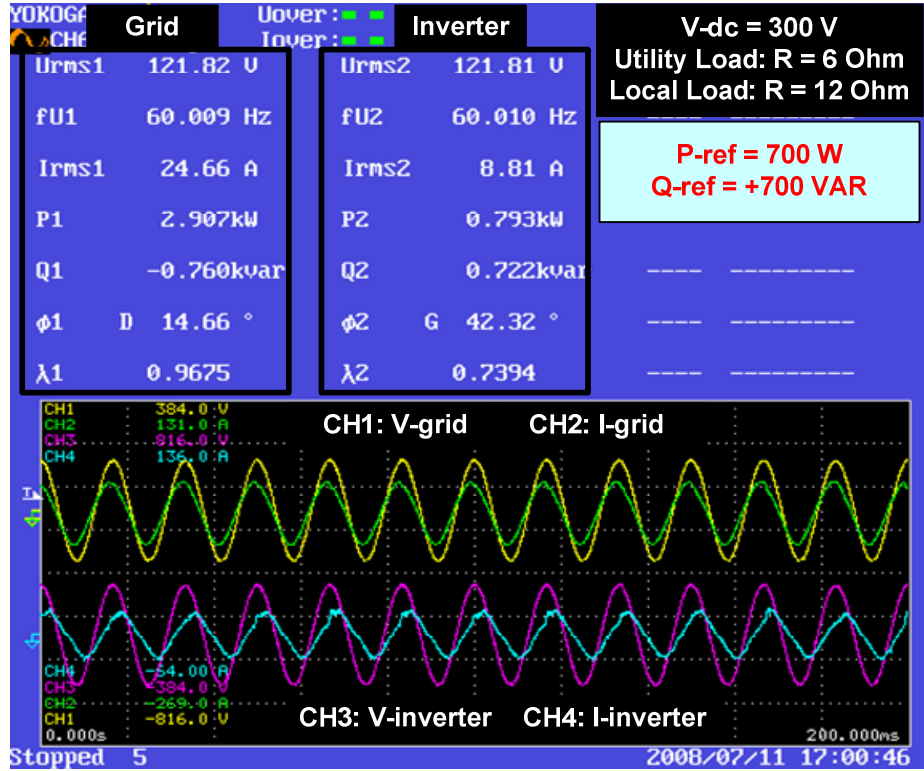
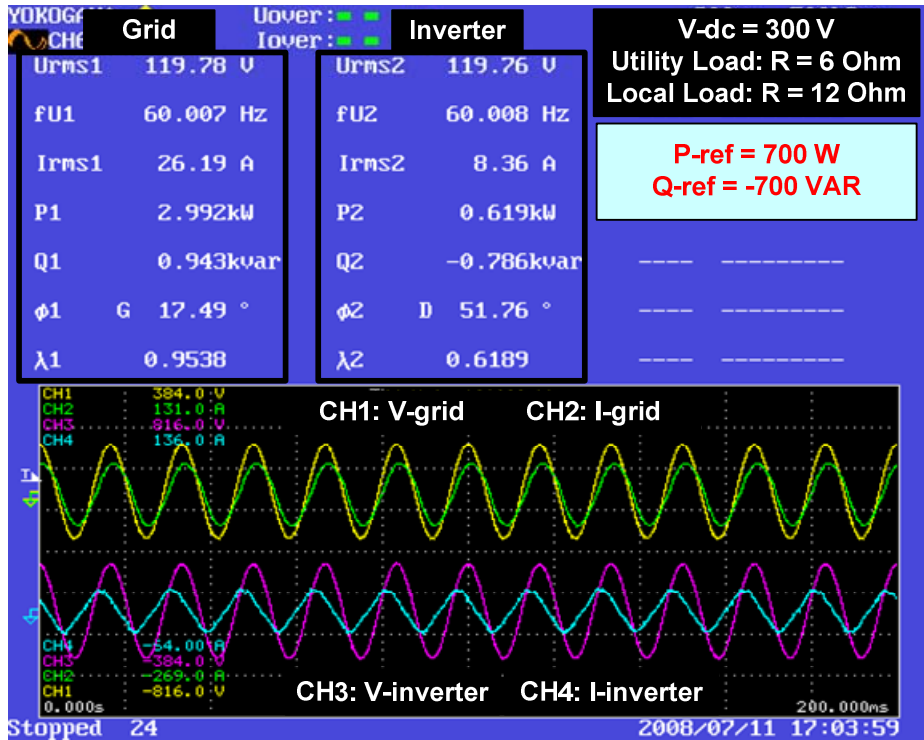


Figure 29. Inverter Power Flow Control (P=0W, Q=1100VAR)



(a)



(b)

Figure 30. Inverter Power Flow Control (P=700W, Q=± 700VAR)

VAR/Voltage Control

As mentioned earlier, for the VAR/voltage control experiment, a 13mH, 20A air-core inductor was placed between the isolation transformer and the grid simulator (see Figure 19). This inductor in series with the grid simulator is an easy way to replicate VAR/voltage drop in the distribution system. Depending on the local load setting, the amount of current flowing through this inductor changes; thus variable VAR drops at the inductor and variable voltage drops at the PCC can be obtained. In the experiment, the inverter was tested for providing a part of the VAR drop, so that the voltage at the PCC remained constant at 120 V AC rms.

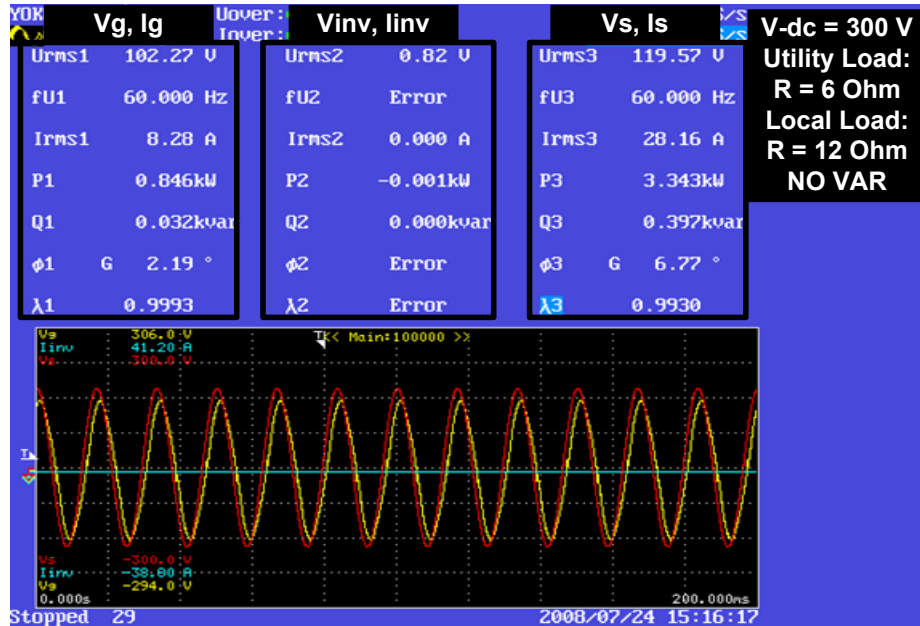
In the VAR/voltage controller, two control loops are used to generate a reference for active power (P_{ref}) and a reference for reactive power (Q_{ref}). The reference rms terminal voltage is compared with the actual output voltage rms and then fed to a proportional controller that outputs Q_{ref} . The DC bus voltage control loop is implemented to obtain P_{ref} . The DC voltage loop helps to provide stability of the VAR controller as well as helps to supply converter losses. From the initial experimental evaluations we have found that using only these proportional controllers is not enough to compensate for the voltage drop. To overcome that problem, offsets are added to the calculated P_{ref} and Q_{ref} . Instead of fixed offsets, these offsets are varied depending on the local load current so that steady-state errors can be minimized. Based on these modified power references, the amplitude and the phase of the reference current waveform are calculated using equations (7) and (8). All these calculations are performed in the slower control loop running at 1/60 s; which means the amplitude and the phase values for the current reference are updated once in each voltage cycle.

Based on the amplitude and phase of the reference current calculated by the slow control loop, the fast 10 kHz interrupt-driven current controller generates the 10 kHz PWM switching pattern. The structure of the current controller is similar to the one as discussed in subsection 4.2.2. Again, the IGBT switches were gated in the bipolar fashion and the DC bus voltage was set at 300V DC. The utility load was set at 6 Ω and the local load was varied to obtain variable VAR drops.

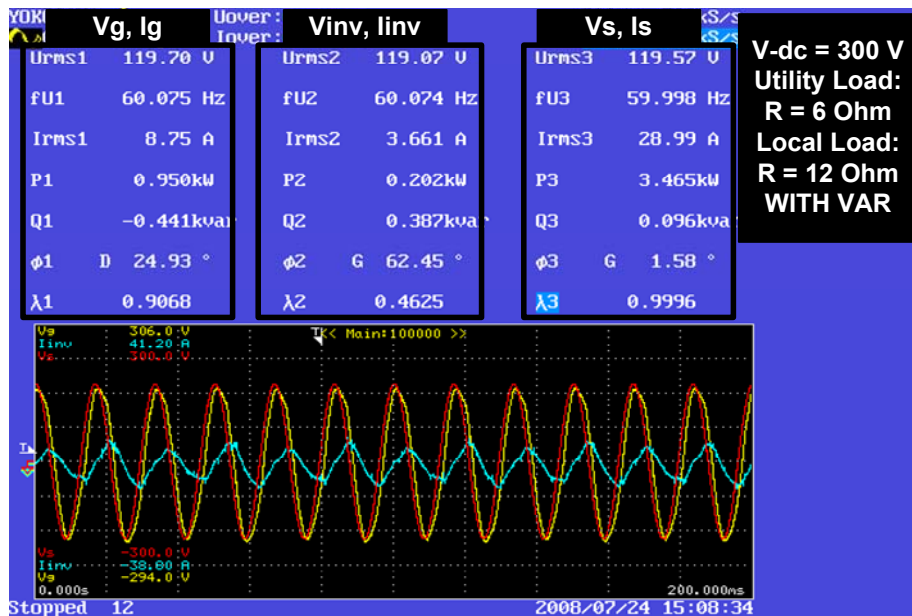
Several experimental case studies were conducted to evaluate the VAR/voltage controller operation. In these case studies, local load resistance has been varied to create different VAR/voltage drops and the inverter is tested for maintaining the PCC voltage for each of the scenarios. Screenshots from the power analyzer for three representative case studies are given in Figure 31 to 33. In each of the figures, the red curve indicates utility voltage, the yellow curve indicates PCC voltage (which is same as the inverter output voltage), and the light blue curve denotes inverter output current. Also in the figure, the measurement values for the scope channels are given, where the first column denotes PCC quantities, followed by inverter quantities in the second column and utility quantities in the third column.

In the first case, local load is set to 12 Ω . The utility and load relays are kept closed. When the inverter is off and the inverter relay is open, the utility is supplying both the loads. Due to VAR drop in the series reactance, the voltage at the PCC drops to 102V AC rms, as can be seen from Figure 31 (a). The reactive power supplied by the utility is around 400VAR lagging. When the inverter is turned on in VAR/voltage control mode, it starts supplying 387VAR to the utility through PCC. The reactive power generated by the inverter causes a drop in reactive power required from the utility and therefore improves the voltage at the

PCC. Under these conditions, the voltage at the PCC increases to around 119V AC rms, as we see in Figure 31 (b). There is a small phase difference between the PCC voltage and utility voltage due to the presence of the series inductor and the isolation transformer leakage reactance.



(a)

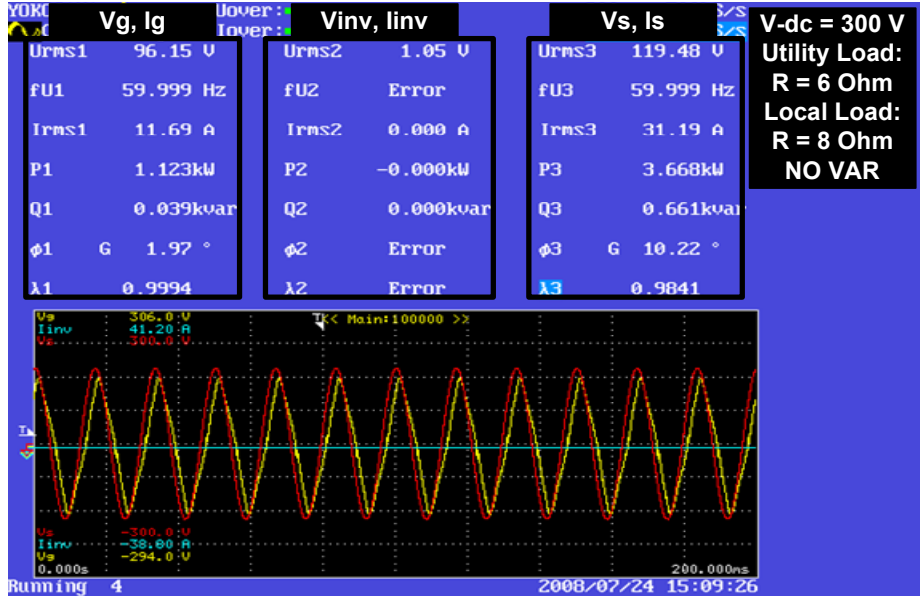


(b)

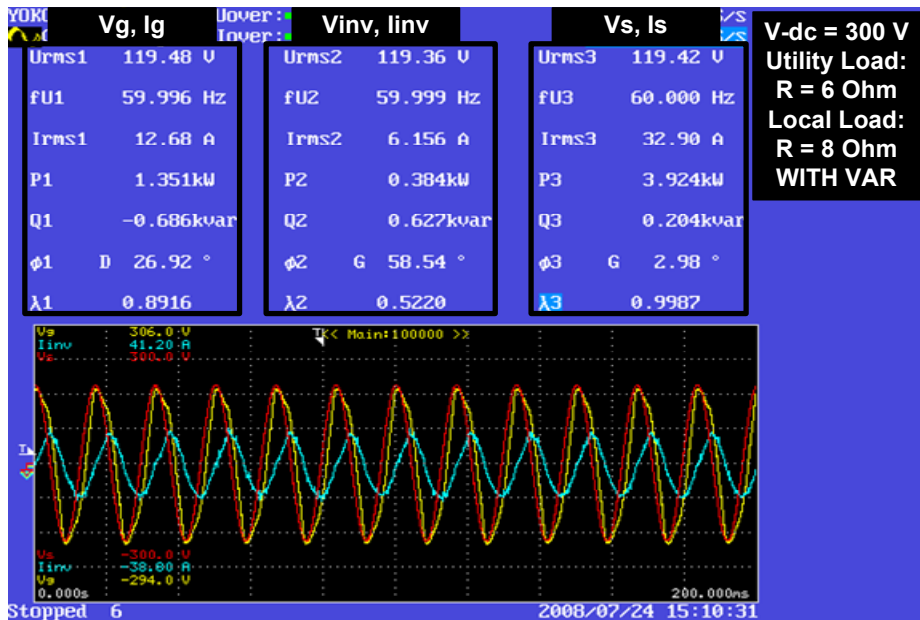
Figure 31. VAR/Voltage Control (Local Load 12 Ohm)

In the second case study, the local load resistance is changed to 8Ω , hence a larger current flows through the series reactance causing a bigger VAR drop. The voltage at PCC in this case is around 96V AC rms when the inverter is not operating, as shown in Figure 32 (a).

When the inverter is turned on, it starts supplying around 600VAR, thus improving the PCC voltage to 119V AC rms. It can also be observed from Figure 32 (b) that the PCC voltage waveform is a little distorted due to low-order harmonics coming from the inverter current. More optimized design of the hardware system components can mitigate this problem.



(a)

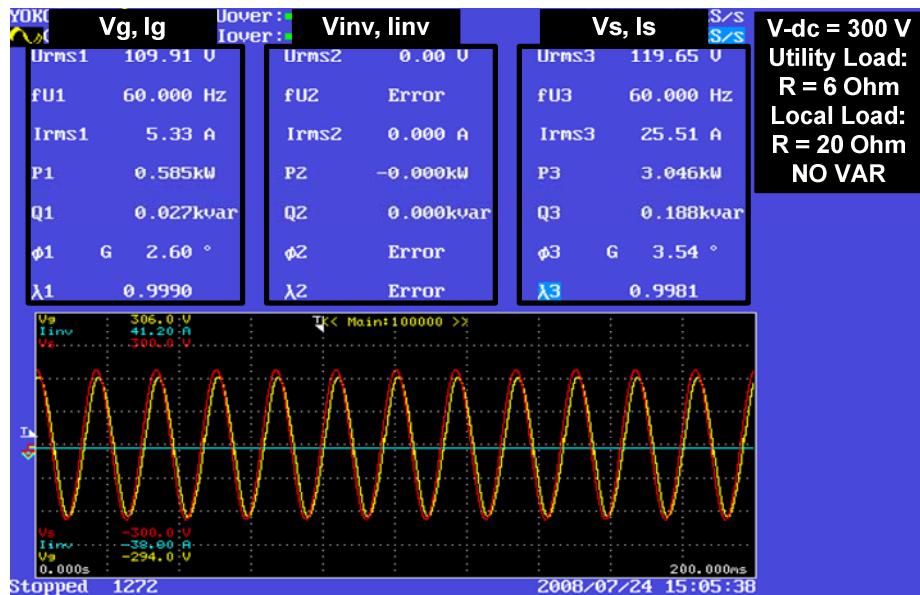


(b)

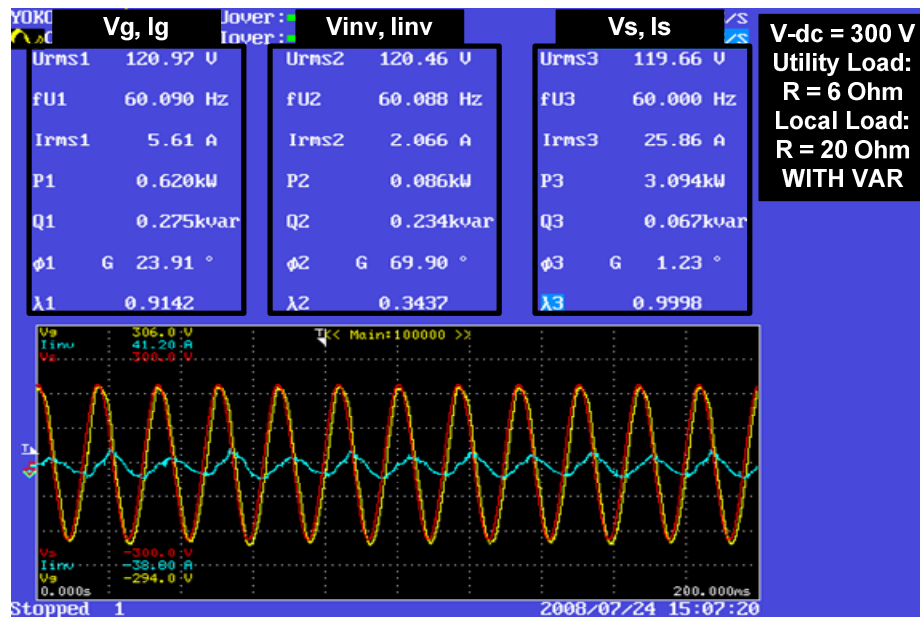
Figure 32. VAR/Voltage Control (Local Load 8 Ohm)

In the third case study, the local load is set to 20Ω. Therefore the VAR drop in the series inductor is less, so the voltage drop will be less. It can be seen from Figure 33 (a) that the voltage at the PCC is now 109V AC rms when the inverter is off. When the inverter is turned on, it starts supplying about 200VAR and improves the PCC voltage to 120V AC rms, as

shown in Figure 33 (b). All three case studies confirm that using the VAR/voltage controller, the inverter is capable of supplying varying amount of VAR to maintain the PCC voltage close to 120V AC rms.



(a)



(b)

Figure 33. VAR/Voltage Control (Local Load 20 Ohm)

5 Rapid Control Prototyping

In the study described in Section 4, all the control codes were written in C-language using Texas Instrument's code composer studio. For the results described in this section, we used Matlab-Simulink toolboxes to self-generate C control codes. Using Simulink's blockset tools the user can model both the power electronics and control algorithms and then generate DSP codes—all in the same development platform. We expect that this interlaced software and firmware design process will, in the future, significantly help in rapid prototyping as the user can first simulate their controls and then can develop the same DSP controls easily for the actual system.

The fast prototyping process described in this report uses TI C2000 series DSP. Simulink uses two toolboxes to program the DSP: Embedded IDE Link for Code Composer Studio (CCS) and Target Support Package TC2. Embedded IDE Link TC2 lets the user to build, test, and verify automatically generated code using MATLAB, Simulink, Real-Time Workshop, and the Code Composer Studio integrated development environment. Embedded IDE Link CC makes it easy to verify code execution within the Code Composer Studio software environment using a model in Simulink software (MathWorks Embedded 2008). Target Support Package TC2 integrates Matlab and Simulink with TI's eXpressDSP tools and C2000 processors (MathWorks Target 2008). Together, these products let the user to develop and validate control designs and DSP algorithms from concept through code by performing automatic code generation, prototyping, and embedded system deployment on C2000 processors.

The same experimental setup as described in Section 4.1 was used. This setup consists of the inverter power and control circuits, DC voltage source, utility grid simulator, RLC load bank, and electronic load bank. The only difference lies in the way the DSP has been programmed. The interrupts, A/D conversion, PLL, inverter control, and PWM generation are all designed in Simulink using Target Support Package TC2 and then compiled and downloaded into the Spectrum Digital eZdsp F2812 evaluation board (Spectrum). Brief descriptions of the control structures and the corresponding experimental results are given later in this section.

5.1 Voltage and Current Control

The islanded voltage control and the utility-connected current control are first developed separately and then combined together in the control model. The complete control structure is shown in Figure 34.

Control Structure

To start with, a target F2812 eZdsp is selected; adding this block to Simulink model provides access to the processor hardware settings that need to be configured to self-generate DSP codes. The processor and target options that can be specified on this block are: processor and board information, memory mapping and layout, allocation of the various code sections, and operating parameters for peripherals on F2812 eZdsp hardware.

The controller was designed so that the control functions are interrupt driven. After completing A/D conversion (ADC), an interrupt is generated and the program goes to the interrupt service routine (ADC-PWM subsystem block). The ADC start occurs based on the

period interrupt of the PWM. Therefore, the interrupt service routine runs once in each PWM cycle and is used to compute duty cycles for the next cycle. For the experimental evaluation, the PWM operates at 10 kHz, therefore the interrupt routine is called at every 100 μ s.

In the main program, the constant denoting the operational mode is fed into an embedded Matlab function block. Based on the input, this block generates two outputs, D_out and Control. The D_out signal is a vector consisting of the status of the analog power-up pin and the on/off status of the three relays (inverter, load, and utility relay). This D_out vector is fed to the digital output block that configures the general-purpose I/O (GPIO) registers to control the GPIO shared pins for digital output. Depending on the control board structure, proper GPIO port and pins are selected so that the analog power is turned on and proper relays can be operated. The Control signal is connected to the ADC-PWM subsystem block and will be discussed later.

A new fixed point PLL was developed which accepts a sinusoidal signal and outputs the phase angle for the input signal. The phase angle output is a ramp signal varying between 0 to 2π and is synchronized on the zero-crossing (rising) of the input signal. The grid voltage signal is fed from the ADC-PWM subsystem block to the PLL and the angle output from PLL is fed back to the same subsystem block. The sample time for the PLL block was set at 0.0003s. As the calculations inside the ADC-PWM subsystem block are done asynchronously with a sample time of 100 μ s defined by the hardware interrupt setting, several rate transition blocks are used in the model. Also the amplitude (Iref_rms) and the phase (Iref_phase) of the current reference are fed into the ADC-PWM subsystem block.

The ADC-PWM subsystem block is a triggered subsystem and activated when the hardware interrupt occurs. Inside this subsystem, DSP's ADC channels are configured to perform analog-to-digital conversion of input signals. Both the ADC module A and B are selected and the simultaneous conversion mode is used. The ADC start occurs based on the period interrupt of the PWM using Event Manager A and an interrupt is posted at the end of the A/D conversion. The output of the ADC goes into the scaling block where the digital signals are converted to their corresponding analog values. These scaled voltage and current measurements along with the PLL-calculated phase angle are then used for the voltage and current controller. The output of the controller is the percentage duty cycle value which is fed to the PWM block to generate 10kHz bipolar PWM switching signals.

When the operational mode is selected as islanded voltage control, the voltage control subsystem is activated. Also during this condition, the inverter relay and the load relay are closed, and the utility relay is kept open. In the voltage control subsystem, as shown in Figure 35, the reference voltage signal is generated first using the phase angle (Theta) information. An offset is added to the PLL-calculated phase angle to take care of the phase shifts produced by sensors and control board filters. The amplitude of the reference voltage is set to 120V AC rms. When a proportional-only controller is used the fixed amplitude of the reference voltage causes large steady-state errors depending on the change in local load. In the previous experimental evaluation section (Section 4), a slower voltage amplitude control loop was used to overcome this problem. This method was used to keep the C-code simple. In the Simulink-based design, a proportional–integral–derivative controller (PID controller) was used in the voltage loop. We chose to use the PID block which is part of the Simulink

C28x digital motor control library; that implements a 32-bit digital PID controller with anti-windup correction. The final output from the voltage control subsystem is the percentage duty cycle and a saturation block was used to limit its output between 5% and 95%.

For the operational mode of utility-connected current control, all three relays were closed and the current control subsystem was activated. Again, frequency and phase of the utility voltage were obtained using the PLL which was then used along with the user-defined phase angle and current amplitude to calculate reference current waveform. The PID controller was finally used to generate percentage duty cycle outputs. The structure of the current control subsystem is given in Figure 36.

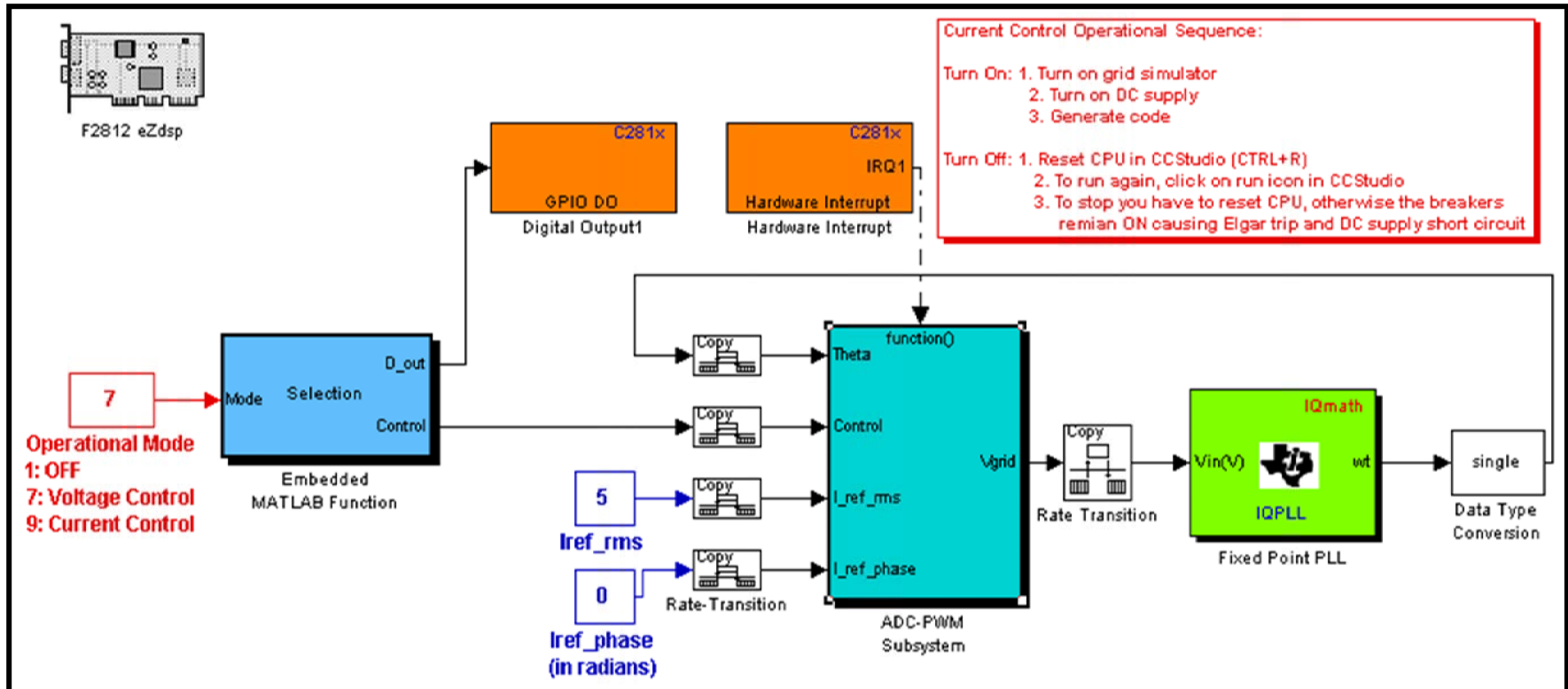


Figure 34. Complete Control Structure for the Voltage and Current Control

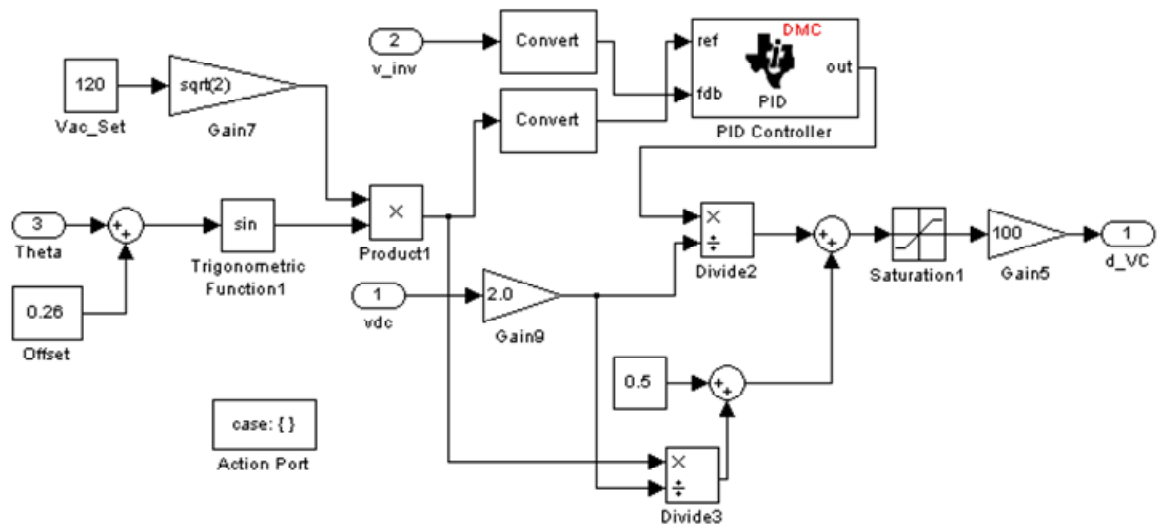


Figure 35. Structure of the Voltage Control Subsystem

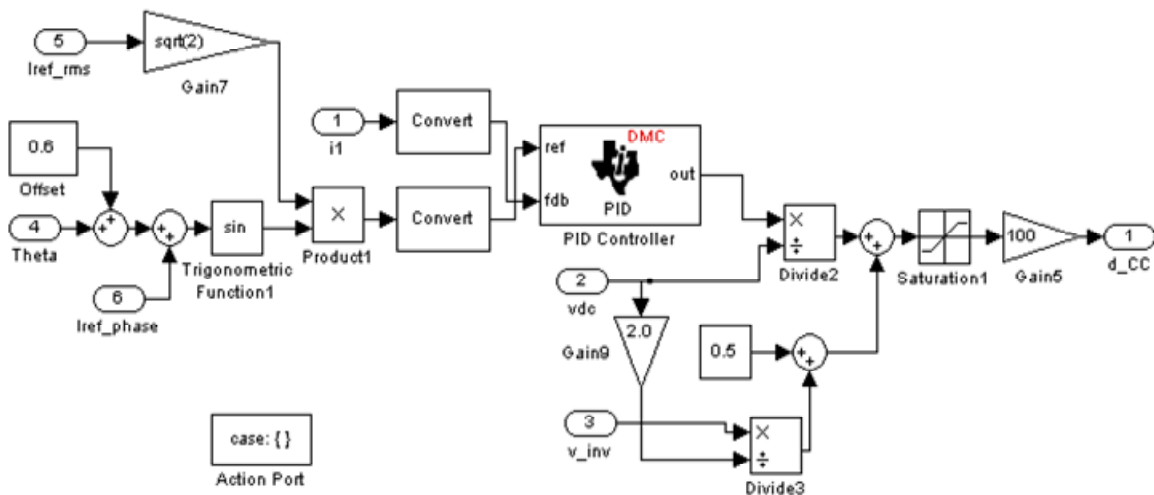


Figure 36. Structure of the Current Control Subsystem

Experimental Results

Researchers used an oscilloscope to observe the voltage and current waveforms and the results are given in Figures 37 to 39. In each of these figures, the utility voltage is the red curve, the inverter voltage curve is in purple, and the inverter output current is in blue.

For the voltage control tests, the DC bus voltage was set at 300V DC and the utility load resistance was set at 6Ω resistive. When the utility relay is left open, the inverter supplies the local load and the utility supplies the utility load. The local load resistance was varied from no load to full load. From Figure 37 and 38, we see that the inverter output voltage operates close to 120V AC rms for both the no load and full load cases. The results for the current control test are given in Figure 39. In this test the DC bus voltage was set at 300V DC, the

utility load was set at 6Ω , and the local load was set at 12Ω . The amplitude of the reference current was set at 9A rms and the phase was set at 50° . It is evident from the figure that the output current follows the reference current with considerable accuracy.

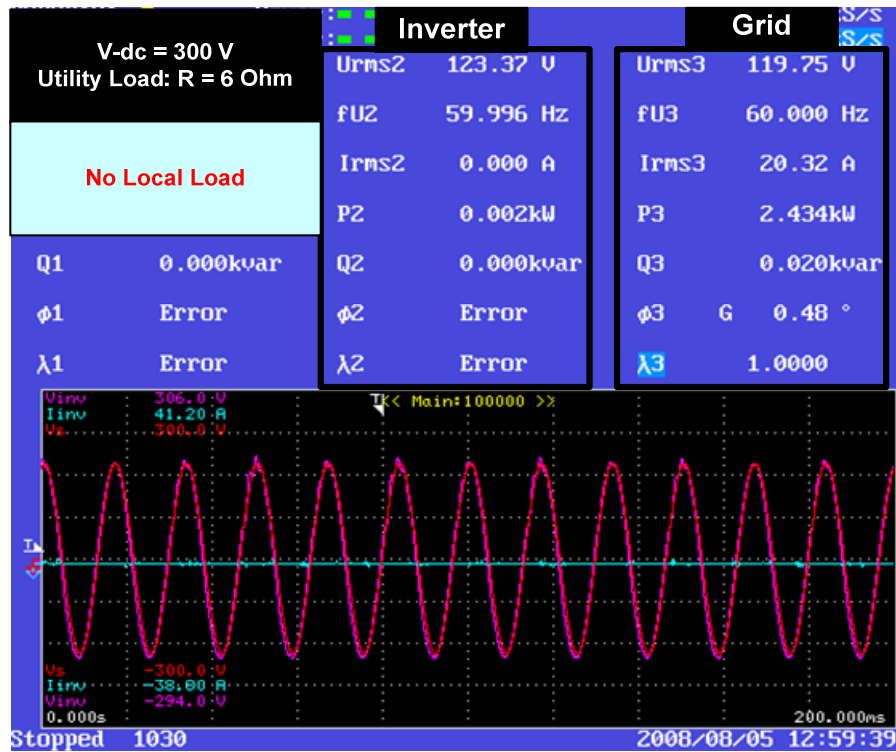


Figure 37. Voltage Control at No Load

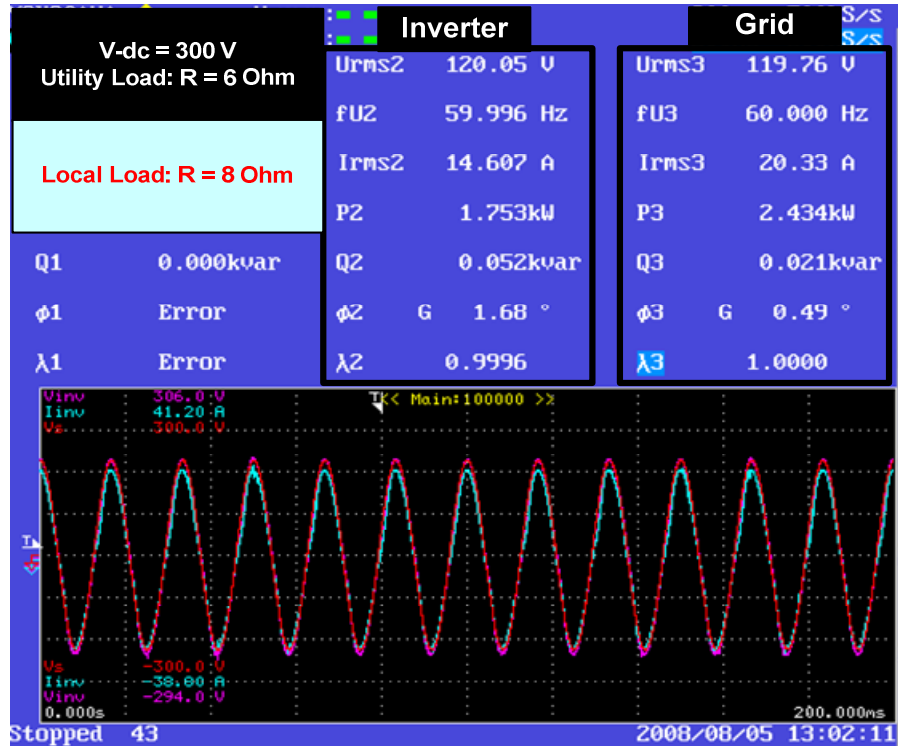


Figure 38. Voltage Control at Full Load

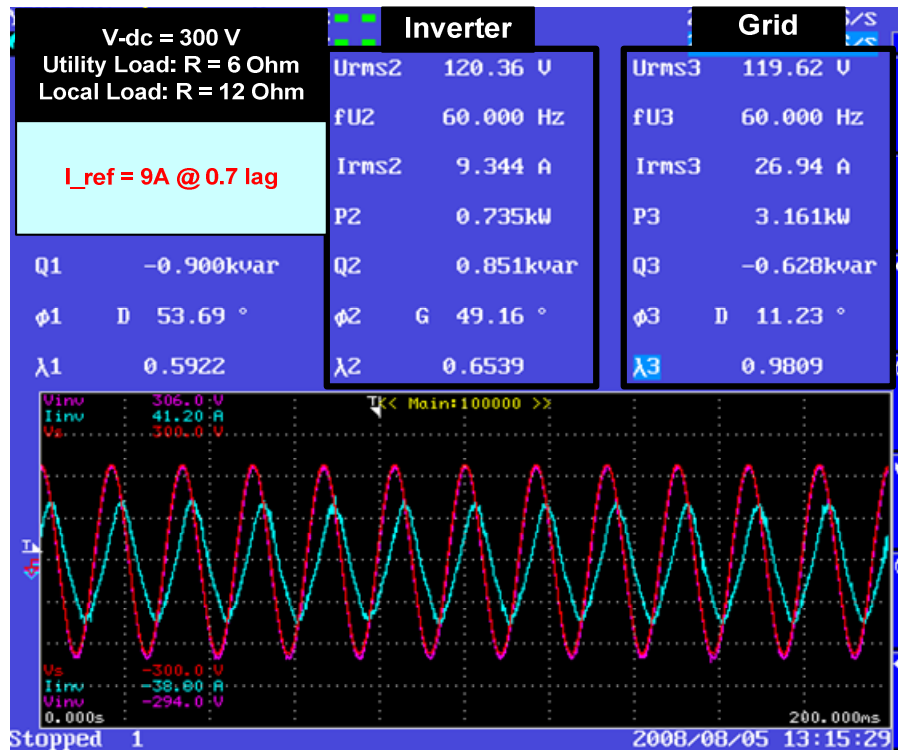


Figure 39. Current Control

5.2 Power Flow Control

The Simulink control diagram for the power flow control is shown in Figure 40. The controller design is similar to the design described in the previous subsection. Instead of the current reference provided by the user, the current reference comes from an outer power calculation loop. These calculated amplitude and phase angle values are then fed into an embedded Matlab function block, where depending on the polarity of the reference reactive power, different scaling gains are used on the calculated current amplitude reference to minimize steady-state errors. The power flow calculations are performed in the slower control loop running at $1/0.0003$ Hz; that means the amplitude and the phase values for the current reference are updated once in every 0.0003s. The structure of the interrupt-driven ADC-PWM subsystem is same as described in the previous subsection.

Results from two experimental case studies for the power flow control are shown in Figures 41 and 42. In those screenshots, the red curve indicates utility voltage, the purple curve indicates inverter voltage, and the light blue curve denotes inverter output current. The DC bus voltage is set at 300V DC. The utility load is set at 6Ω and the local load is set at 15Ω . The power analyzer screenshot for the case when active power reference (P_{ref}) is set to 800W and reactive power reference (Q_{ref}) is set to -800VAR is given in Figure 41. For this power flow condition, the expected amplitude and phase of the output current is 9.43A and 45° lead respectively. It can be observed from the figure that the inverter output current rms and phase are close to the expected values. In the second case study, P_{ref} is set to 900W and Q_{ref} is set to 800VAR. Again the inverter output powers, as evident from Figure 42, follow the reference powers closely.

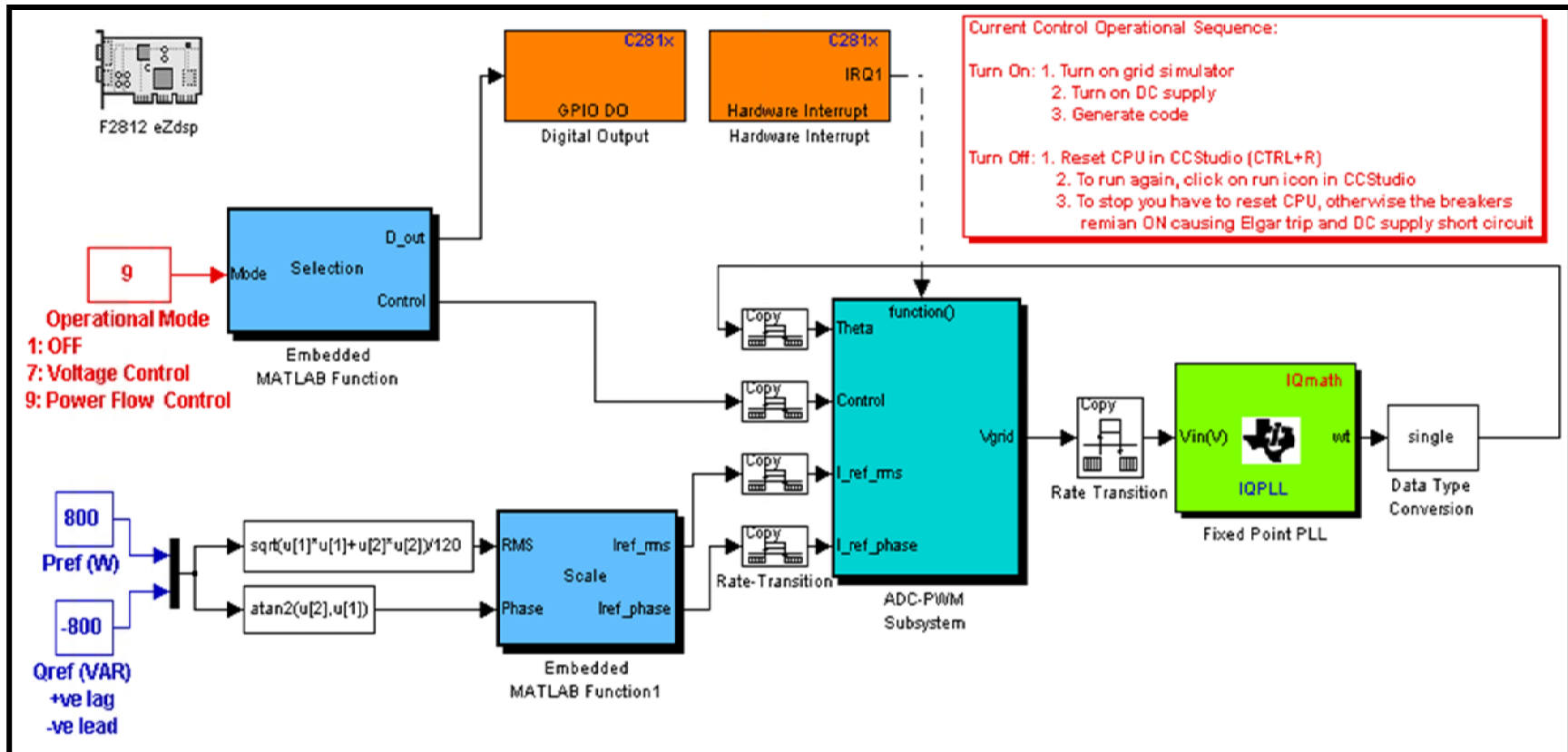


Figure 40. Complete Control Structure for the Voltage and Power Flow Control

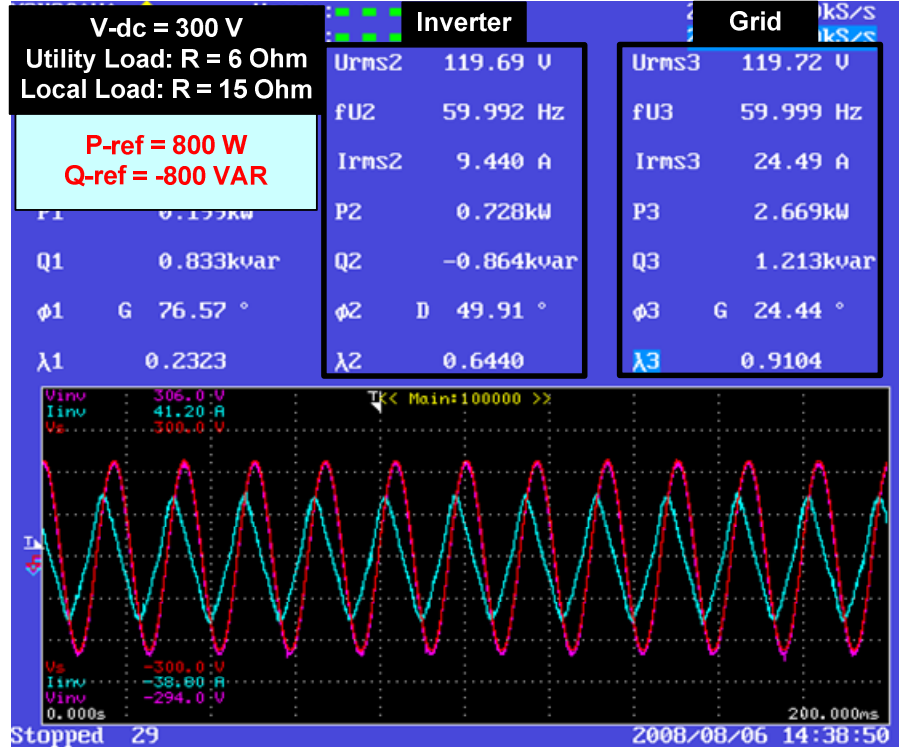


Figure 41. Power Flow Control (P=800W, Q=-800VAR)

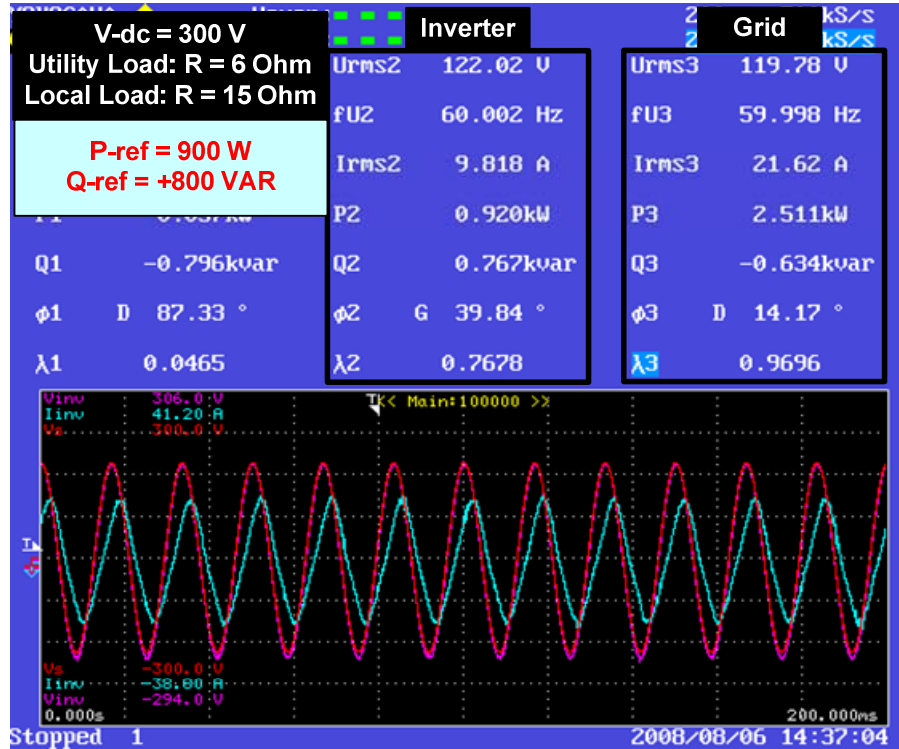


Figure 42. Power Flow Control (P=900W, Q=800VAR)

5.3 VAR/Voltage Control

As mentioned before, for the VAR/voltage control experiment, a 13mH, 20A air-core inductor was placed between the isolation transformer and the grid simulator (Figure 19). The Simulink control structure for VAR/voltage control is given in Figure 43. In the VAR/voltage controller, two control loops were used to generate reference active power (P_{ref}) and reference reactive power (Q_{ref}). The reference rms terminal voltage was compared with the actual output voltage rms and then fed to a proportional controller that outputs Q_{ref} . The DC bus voltage control loop was implemented to obtain P_{ref} . Fixed offsets were added to the calculated P_{ref} and Q_{ref} to reduce steady-state errors. Based on these modified power references, the amplitude and the phase of the reference current waveform were calculated using equations (7) and (8). All these calculations are performed in the slower control loop running at $1/0.0003$ Hz; that means the amplitude and the phase values for the current reference are updated once in every 0.0003s. The structure of the interrupt-driven ADC-PWM subsystem is same as described in the Section 5.1.1.

Several experimental case studies were conducted to evaluate the VAR/voltage controller operation. In these case studies, the DC bus voltage was set at 300V DC and the utility load was set at 6Ω . The local load resistance was varied to create different VAR/voltage drop and inverter was tested for maintaining the PCC voltage for each of the scenarios. The power analyzer screenshot from a representative case study is shown in Figure 44, where the local load resistance is set to 10Ω . In the figure, the red curve indicates utility voltage, the yellow curve indicates PCC voltage (which is same as the inverter output voltage), and the light blue curve denotes inverter output current.

When the inverter is off and the inverter relay is open, the utility is supplying both the loads, and due to VAR drop in the series reactance, the voltage at the PCC drops to 99V AC rms, as can be seen from Figure 44 (a). When the inverter is turned on in VAR/voltage control mode, it starts supplying VAR to the utility through PCC. During this condition, the voltage at the PCC increases to 118V AC rms, as can be observed in Figure 44 (b). There is a small phase difference between the PCC voltage and utility voltage due to the presence of the series inductor and the isolation transformer leakage reactance.

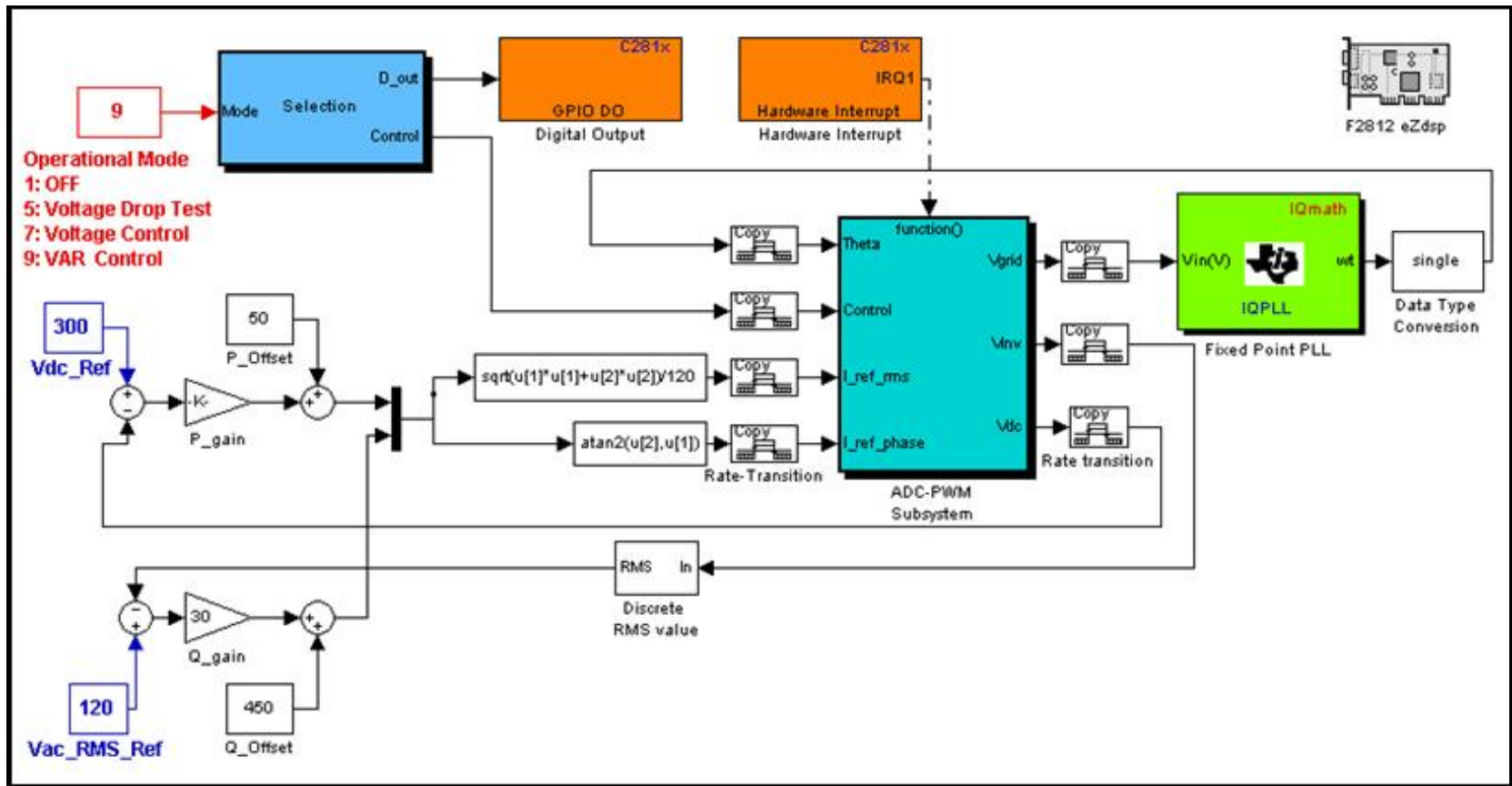
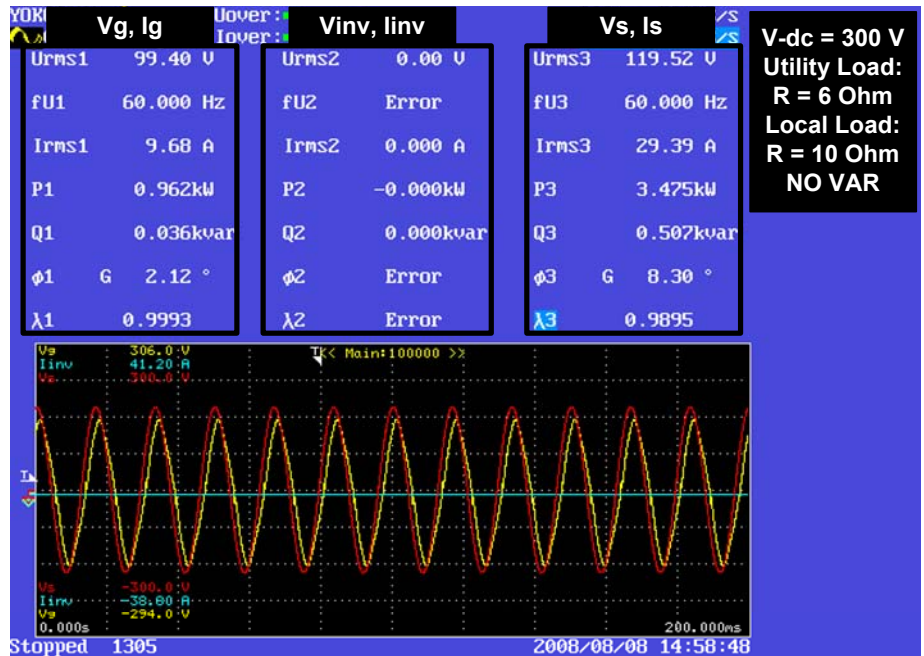
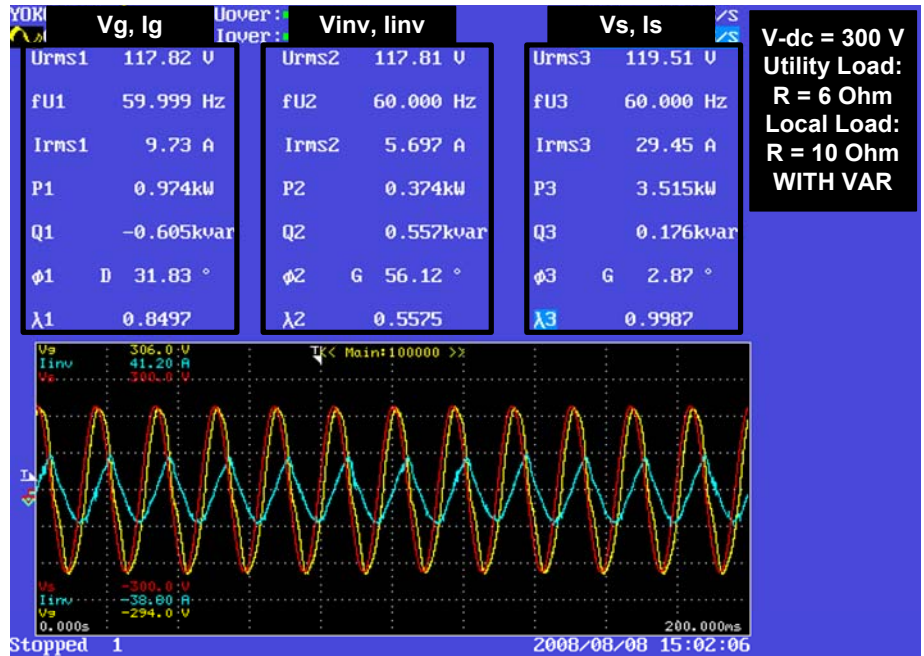


Figure 43. Complete Control Structure for the Voltage and VAR Control



(a)



(b)

Figure 44. VAR/Voltage Control (Local Load 10 Ohm)

6 Conclusion

For energy sources such as PV or fuel cell that generate DC, an inverter is required to convert DC into AC for utility connection and consumer use. Though low power single-phase inverters are very common and available from different manufacturers, these commercial inverters mainly work as a controlled current source when they are operating in the utility-connected mode. “Development of Standardized Power Electronic Components, Subsystems, and Systems for Increased Modularity and Scalability (Chakraborty et al. 2007), provides the details of the design and some initial testing of the NREL-developed inverter platform and “Advanced Power Electronic Interfaces for Distributed Energy Systems Part 1: Systems and Topologies” (Kramer et al. 2008) outlines the typical topologies could be used for DE and renewable energy applications. This report outlines the detailed modeling, design, and testing of a single phase DC to AC inverter that operates in both islanded mode and utility-connected mode. Both modeling and experimental results are given to demonstrate the ability of the developed inverter to provide advanced control functions such as power flow and VAR/voltage regulation.

We used the Simulink software platform to develop the single-phase inverter model and the control algorithms before they were implemented in hardware. The parameters and simulation conditions for the model were carefully selected to accurately emulate the hardware. Also, the control designs have been developed in such a way that they could be implemented on a hardware DSP platform. Though IEEE 1547 currently does not allow active voltage control by the DE sources, the simulation results presented in this report confirm that with modification to the current control, the DE inverter can be designed to supply reactive power and regulate VAR/voltage at the PCC, which can be beneficial to the electric power distribution system.

All the control functions were experimentally evaluated using the inverter platform consisting of a Semikron SKAI module and a Spectrum Digital's F2812 eZdsp controller. In addition to the inverter power and control circuits, the laboratory test setup consisted of several other components, such as a DC voltage source, a utility grid simulator, a RLC load bank, and an electronic load bank. Two techniques were demonstrated for DSP code generation. Initially the DSP code was written in C- language using Code Composer Studio. In later stage of the research, the Simulink DSP toolbox was used to self-generate code for the DSP. Irrespective of the method used for code generation, experimental results proved that the inverter successfully operates for all functional modes, namely the islanded voltage control mode, and utility-connected current control, power flow control, and VAR/voltage control modes. The successful tests using Simulink self-generated DSP codes show promise for fast prototyping of power electronics controls.

Future work will concentrate on developing and testing additional ancillary functions such as power quality control and seamless transfer for the inverter associated with DE sources. Also the Simulink DSP toolbox will be explored and used to develop useful software and firmware libraries. We expect that this methodology will reduce the time to develop prototypes and will help the designers to develop advanced control schemes for their DE power electronics.

References

Barker, P.P.; De Mello, R.W. (July 2000). "Determining the Impact of Distributed Generation on Power Systems. I. Radial Distribution Systems." IEEE Power Engineering Society Summer Meeting.

Campbell, J.B.; King, T.J.; Ozpineci, B.; Rizy, D.T.; Tolbert, L.M.; Xu, Y.; Yu, X. (December 2005). "Ancillary Services Provided from DER." ORNL, ORNL/TM-2005/263.

Chakraborty, S.; Pink, C.; Price, J.; Kroposki, B.; Kern, G. (November 2007). "Development of Standardized Power Electronic Components, Subsystems, and Systems for Increased Modularity and Scalability." NREL/TP-581-42412.

Elgar (2008). "SmartWave AC Power Source MODELS SW 10500 SW 15750 SW 21000." M162002-01 rev D.

Hingorani, N.G.; Gyugyi, L. (2000). Understanding FACTS: Concepts and Technology of Flexible AC Transmission Systems. Wiley-IEEE Press.

Institute of Electrical and Electronics Engineers, Inc. (July 2003). "IEEE Standard for Interconnecting Distributed Resources to Electric Power Systems." IEEE Standard 1547-2003. Piscataway NJ: IEEE.

Kramer, W.; Chakraborty, S.; Kroposki, B.; Thomas, H. (March 2008). "Advanced Power Electronic Interfaces for Distributed Energy Systems Part 1: Systems and Topologies." NREL/TP-581-42672.

Kroposki, B.; Pink, C.; DeBlasio, R.; Thomas, H.; Simoes, M.; Sen, P.K. (June 2006). "Benefits of Power Electronic Interfaces for Distributed Energy Systems." IEEE Power Engineering Society General Meeting.

Mariun, N.; Masdi, H.; Bashi, S.M.; Mohamed, A.; Yusuf, S. (April 2006). "Design of a Prototype D-STATCOM using DSPCcontroller for Voltage Sag Mitigation." IEEE Power India Conference.

MathWorks "Embedded IDE Link CC (for TI's Code Composer Studio)." (2008). <http://www.MathWorks.com/products/ccslink>. Accessed October 15, 2008.

MathWorks "SimPowerSystems." (2008). <http://www.MathWorks.com/products/simpower>. Accessed September 2008.

MathWorks "Simulink." (2008). <http://www.MathWorks.com/products/simulink>. Accessed September 2008.

MathWorks "Target Support Package TC2 (for TI's C2000 DSP)." (2008). <http://www.MathWorks.com/products/tic2000>. Accessed October 1, 2008.

Mohan, N.; Undeland, T.M.; Robbins, W.P. (2003). *Power Electronics: Converters, Applications, and Design*. John Wiley & Sons, Inc.

National Electrical Manufacturers Association. (1985). "ANSI C84.1-1995 Electrical Power Systems and Equipment - Voltage Ratings (60Hz)."

Rahmati, A.; Abrishamifar, A.; Abiri, E. (December 2006). "An DSTATCOM for Compensating Different Abnormal Line Voltage and Nonlinear Load." IEEE International Conference on Industrial Technology.

Semikron. *SKAI-HV Users Manual*.

Spectrum Digital. <http://www.spectrumdigital.com>. Accessed September 2008.

Texas Instruments. "Code Composer Studio IDE." <http://www.ti.com>. Accessed October 2008.

Twining, E.; Holmes, D.G. (June 2003). "Voltage Compensation in Weak Distribution Networks using Multiple Shunt Connected Voltage Source Inverters." IEEE Power Tech Conference, June 2003.

Yokogawa. "PZ4000 Power Analyzer User Manual." IM 253710-01E, 2nd ed.

REPORT DOCUMENTATION PAGE

Form Approved
OMB No. 0704-0188

The public reporting burden for this collection of information is estimated to average 1 hour per response, including the time for reviewing instructions, searching existing data sources, gathering and maintaining the data needed, and completing and reviewing the collection of information. Send comments regarding this burden estimate or any other aspect of this collection of information, including suggestions for reducing the burden, to Department of Defense, Executive Services and Communications Directorate (0704-0188). Respondents should be aware that notwithstanding any other provision of law, no person shall be subject to any penalty for failing to comply with a collection of information if it does not display a currently valid OMB control number.

PLEASE DO NOT RETURN YOUR FORM TO THE ABOVE ORGANIZATION.

1. REPORT DATE (DD-MM-YYYY) November 2008			2. REPORT TYPE Technical Report		3. DATES COVERED (From - To)	
4. TITLE AND SUBTITLE Advanced Power Electronic Interfaces for Distributed Energy Systems Part 2: Modeling, Development, and Experimental Evaluation of Advanced Control Functions for Single-Phase Utility-Connected Inverter				5a. CONTRACT NUMBER DE-AC36-08-GO28308		
				5b. GRANT NUMBER		
				5c. PROGRAM ELEMENT NUMBER		
6. AUTHOR(S) S. Chakaborty, B. Kroposki, and W. Kramer				5d. PROJECT NUMBER NREL/TP-550-44313		
				5e. TASK NUMBER WW2C.1000		
				5f. WORK UNIT NUMBER		
7. PERFORMING ORGANIZATION NAME(S) AND ADDRESS(ES) National Renewable Energy Laboratory 1617 Cole Blvd. Golden, CO 80401-3393				8. PERFORMING ORGANIZATION REPORT NUMBER NREL/TP-550-44313		
9. SPONSORING/MONITORING AGENCY NAME(S) AND ADDRESS(ES)				10. SPONSOR/MONITOR'S ACRONYM(S) NREL		
				11. SPONSORING/MONITORING AGENCY REPORT NUMBER		
12. DISTRIBUTION AVAILABILITY STATEMENT National Technical Information Service U.S. Department of Commerce 5285 Port Royal Road Springfield, VA 22161						
13. SUPPLEMENTARY NOTES						
14. ABSTRACT (Maximum 200 Words) Integrating renewable energy and distributed generations into the Smart Grid architecture requires power electronic (PE) for energy conversion. The key to reaching successful Smart Grid implementation is to develop interoperable, intelligent, and advanced PE technology that improves and accelerates the use of distributed energy resource systems. This report describes the simulation, design, and testing of a single-phase DC-to-AC inverter developed to operate in both islanded and utility-connected mode. It provides results on both the simulations and the experiments conducted, demonstrating the ability of the inverter to provide advanced control functions such as power flow and VAR/voltage regulation. This report also analyzes two different techniques used for digital signal processor (DSP) code generation. Initially, the DSP code was written in C programming language using Texas Instrument's Code Composer Studio. In a later stage of the research, the Simulink DSP toolbox was used to self-generate code for the DSP. The successful tests using Simulink self-generated DSP codes show promise for fast prototyping of PE controls.						
15. SUBJECT TERMS power electronics; advanced power electronic interface; distributed energy; topology; electric power distribution; advanced controls; inverter; Simulink; SmartGrid						
16. SECURITY CLASSIFICATION OF:			17. LIMITATION OF ABSTRACT UL	18. NUMBER OF PAGES	19a. NAME OF RESPONSIBLE PERSON	
a. REPORT Unclassified	b. ABSTRACT Unclassified	c. THIS PAGE Unclassified			19b. TELEPHONE NUMBER (Include area code)	